MSFC

IITRI M6123

ABSOLUTE PRESSURE TRANSDUCER CALIBRATION DEVICE

by

D. F. Pernet

Prepared for

NATIONAL AERONAUTICS AND SPACE ADMINISTRATION

CONTRACT NO. NAS8-11915

July 1966

IIT RESEARCH INSTITUTE

IITRI M6123

FINAL REPORT

ABSOLUTE PRESSURE TRANSDUCER CALIBRATION DEVICE

by

D. F. Pernet

Prepared for

NATIONAL AERONAUTICS AND SPACE ADMINISTRATION

July 1966

CONTRACT NO. NAS8-11915 (DCN 1-5-75-00085 and S1)

Technical Management
NASA George C. Marshall Space Flight Center
Instrument Development Section
B. H. Neighbors

IIT Research Institute
Chicago, Illinois 60616

FOREWORD

"Absolute Pressure Transducer Calibration Device" was undertaken for NASA George C. Marshall Space Flight Center, Contract No. NAS8-11915, DCN 1-5-75-00085 and S1, by the IIT Research Institute, Chicago, Illinois, Project No. M6123 (originally N6132). The project leader was D. F. Pernet, responsible for the direction of the work and author of this report. The author wishes to acknowledge the valuable contributions to the program of C. S. Caccavari and G. L. Johnson, especially for their contributions in developing the sound generator system and the interferometer, respectively. Acknowledgements are also extended to W. E. Lawrie and A. J. Montgomery for their valuable advice.

ABSTRACT

An instrument has been developed to calibrate high intensity, high frequency transducers. The device consists of two horn-driver units and a St. Clair generator, which generate sound pressure levels in an acoustic cavity of between 140 and 175 db in the frequency range 500 c/s to 40 kc/s, together with an optical interferometer using a helium neon laser source. The acoustic cavity is located in one of the two beams of a Michelson interferometer. The sound field in the cavity produces a temporal variation in the optical interference distribution. This variation is monitored with a photodiode detector. The magnitude and phase of the sound pressure field in the cavity can be determined by a simple method of signal processing enabling the pressure sensitivity as well as the phase characteristics of transducers to be determined. Using this instrument, the sensitivity of a 1/4 in. condenser microphone was determined. The results agreed to better than 1/2 db with those of a pistonphone calibration.

TABLE OF CONTENTS

LIST OF FIGURES

LIST OF FIGURES (Continued)

I. INTRODUCTION AND SUMMARY

Transducers which are used to monitor acoustic or aerodynamic pressure fields can give only a qualitative indication of these fields if they have not been calibrated. Understandably, considerable attention has been given to the problem of transducer calibration to enable quantitative analyses of pressure fields to be made.

In this study we have developed an absolute pressure calibration device designed specifically to calibrate high intensity, wide frequency-response transducers. This device enables pressure sensitivity as well as phase characteristics of transducers to be determined. Normally, phase information contained in acoustic or aerodynamic pressure fields becomes redundant in signal analysis. Consequently, conventional methods of transducer calibration seldom provide (and in many instances are incapable of providing) information about the phase characteristics of transducers. However, when, in experimental acoustic or aerodynamic studies, one or several transducers' signal outputs are to be auto- or cross-correlated, respectively, it is essential that the phase characteristics of the transducers be known. Consequently, in our approach to the problem, we have been aware of this additional requirement for the device.

The calibration device developed in this study uses an optical interferometer to establish the absolute pressure amplitude of the calibrating signal. The interferometer is of

the Michelson type and incorporates the acoustic cavity in one of the two optical beam paths. The density fluctuations in the acoustic cavity, which are associated with the pressure fluctuations of the calibrating acoustic signal, produce a time-varying optical interference distribution. This distribution is monitored with a photodiode detector. The output signal of the optical detector enables determination of both magnitude and phase information on the pressure fluctuations in the acoustic cavity.

Comparison of this data to that of the electrical output signal of a transducer located in the cavity enables the sensitivity and phase characteristics of the transducer to be determined.

The requirement that the calibration device be capable of calibrating transducers at high intensities over a wide frequency range posed several acoustical problems. Several types of acoustic generator were examined to determine their capabilities. The acoustic signal generation in the final device is provided by three interchangeable units; two horn-drivers for frequencies up to 16 kc/s and a St. Clair generator for frequencies beyond 20 kc/s. The acoustic energy produced by these devices is propagated into a 1/4 in. diameter telescopic tube at the end of which the 1/4 in. transducers (which are to be calibrated) are located. Adjustment of the length of the 1/4 in. tube allows longitudinal tuning of the cavity, which produces increased level at the location of the transducer

diaphragm when additional signal level is required. Because longitudinal pressure gradients will exist in the tube, the optical beam scans the cavity in a transverse direction immediately in front of the transducer diaphragm for minimal error in calibration.

The system is capable of being operated under reduced pressure or filled with gases other than air. Using this device to check the calibration of a 1/4 in. Bruel and Kjaer condenser microphone, the agreement between the manufacturer's specification and that obtained using the calibration device was better than 1/2 db at calibration levels in the range 140 to 175 db over a frequency range 520 c/s to 24 kc/s.

II. ACOUSTIC GENERATOR SYSTEM

The design of an acoustic generator system which would operate from 100 c/s to 40 kc/s and produce in a cavity sound pressure levels as high as 180 db at ambient pressures of both one atmosphere and 1/3 atmosphere posed many problems.

Since it is beyond the state of the art to produce in the laboratory, using a single acoustic generator, pure tone signals meeting these specifications, it was necessary to investigate the potential of several types of high intensity acoustic generators. In addition, it was necessary to investigate the potential of several types of high intensity acoustic generators. In addition, it was necessary to investigate the propagation of high frequency sound in tubes and cavities containing either air or helium.

In this section of the report, the results of these investigations are described briefly. Emphasis is given only to those results having significant bearing on the final design of the transducer calibration system.

Low Frequency Generators

The first step in this phase of the program was to procure commercially available sound sources and determine their sound outputs in the frequency range of interest. Many domestic and foreign loudspeaker manufacturers were approached, but only a few produced devices whose specifications indicated

a potential usefulness. Several horn-driver units were purchased and their characteristics, as supplied by the manufacturer, are listed in Table I.

Each horn-driver was coupled to a 1/4 in. diameter tube and the sound pressure level in the tube was determined at several frequencies when the driver unit was operated at half its rated power handling capacity. The system used is shown in Fig. 1. It is generally considered that when horn-drivers are operated with steady sinusoidal signals, the power input should not exceed this given value.

Figure 2 shows a composite of the sound pressure levels generated in the 1/4 in. diameter tube for each of the horn-drivers investigated. From this data it can be seen that maximum sound pressure levels can be obtained in the tube using only two units; the Jensen DD-100A and the James B. Lansing 075. The Jensen DD-100A covers the frequency range from 500 c/s to 4 kc/s and the James B. Lansing 075 covers the range from 4 kc/s to 16 kc/s. It can be seen from Fig. 2 that although the latter unit operates to frequencies beyond 50 kc/s, it does not produce the sound pressure levels which are required for the transducer calibration system.

These two horn-driver units are used in the final system to generate acoustic signals to a frequency of 16 kc/s. Individual coupling adapters were constructed to couple these units to the acoustic cavity. The Jensen DD-100A unit was enclosed in a strong, close-fitting, airtight plastic bag to

TABLE I

MANUFACTURERS SPECIFICATIONS OF PURCHASED HORN-DRIVER UNITS

Manufacturer	Type	Impedance (ohms)	Peak Power (Watts)	Frequency Response (cps)	Approx. Half Peak Power Voltage
Electro-Voice	T35	16	40	3,500 to 40,000	18
James B. Lansing	075	16	20	2,500 to 4,000	13
University	SA-30	16	30	90 to 10,000	16
Electro-Voice	T25A	16	30	700 to 13,000	16
Jensen	D-40	16	40	100 to 5,000	18
Jensen	DD-100A	50/(12.5)	100	100 to 5,000	50

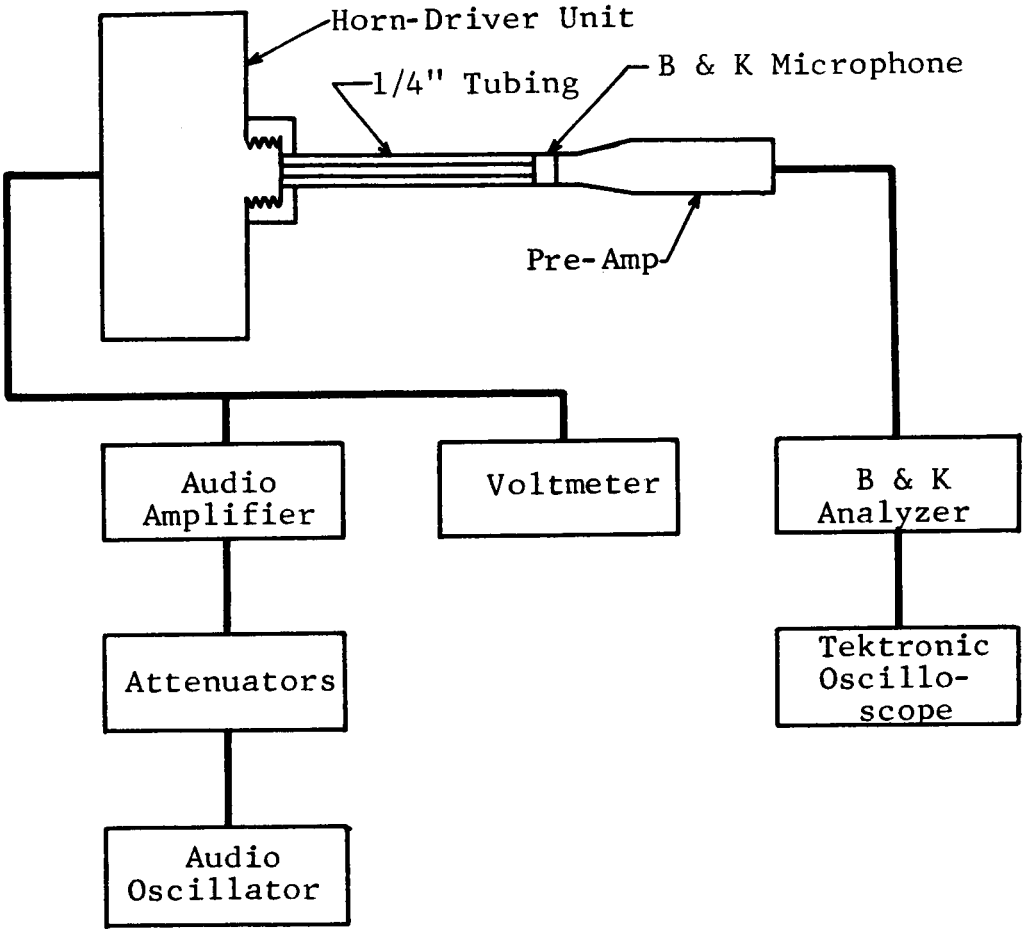

Fig. 1. Block Diagram for Measuring the Acoustic Signal Generated in a 1/4 in. Diameter Tube by Horn-Driver Units.

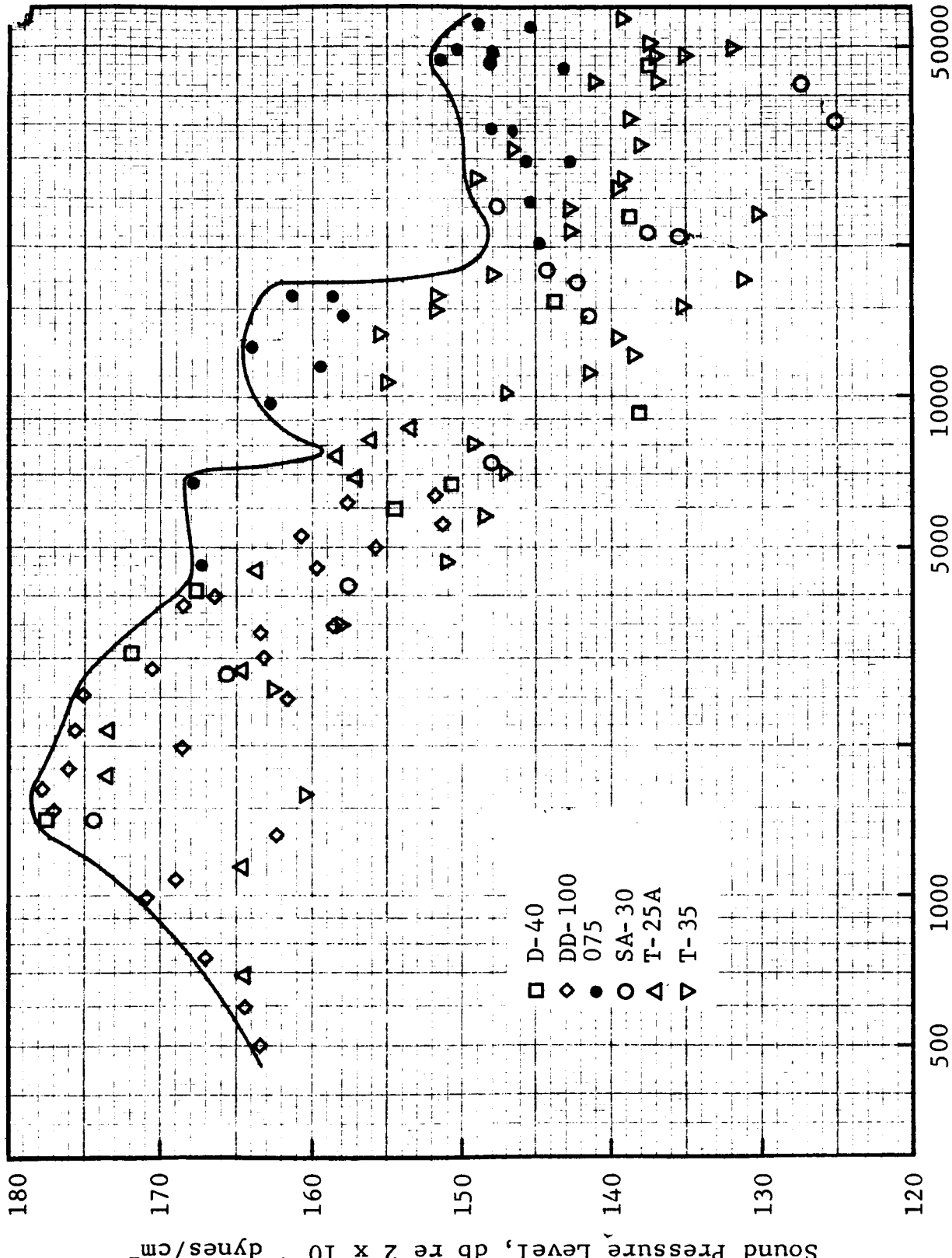

Fig. 2. Composite of Sound Pressure Levels Generated in 1/4 in. Diameter Tubing for Each Horn-Driver Unit.

enable the unit to be operated at reduced pressures. The Lansing 075 unit, being airtight, required no modification to enable reduced pressure operation.

High Frequency Generators

To generate high frequency acoustic signals, three types of device were investigated: magnetostrictive transducers, Friedmann horns, and St. Clair generators. Unlike the low frequency horn-driver units, these three types of transducer are resonant devices and consequently have a limited capability. However, no alternative broad-band devices are currently available to meet the desired specifications and since the frequency range between 16 kc/s and 40 kc/s need only be covered at one-third octave intervals, the use of resonant devices was not considered unduly inconvenient.

The first sound generator which was investigated was a magnetostrictive transducer (Ref. 1), resonant at 14.5 kc/s. This transducer was chosen because of its availability and the minimal shop time which would be required to have it operational. The transducer was constructed from stamped nickel window laminations, which are annealed to oxidize the surfaces to provide insulation and are finally epoxy-bonded together to form a stack. The transducer was bolted to a half-wavelength stub which also serves as a support mechanism as shown in Fig. 3. A displacement transformer was bolted to the stub and

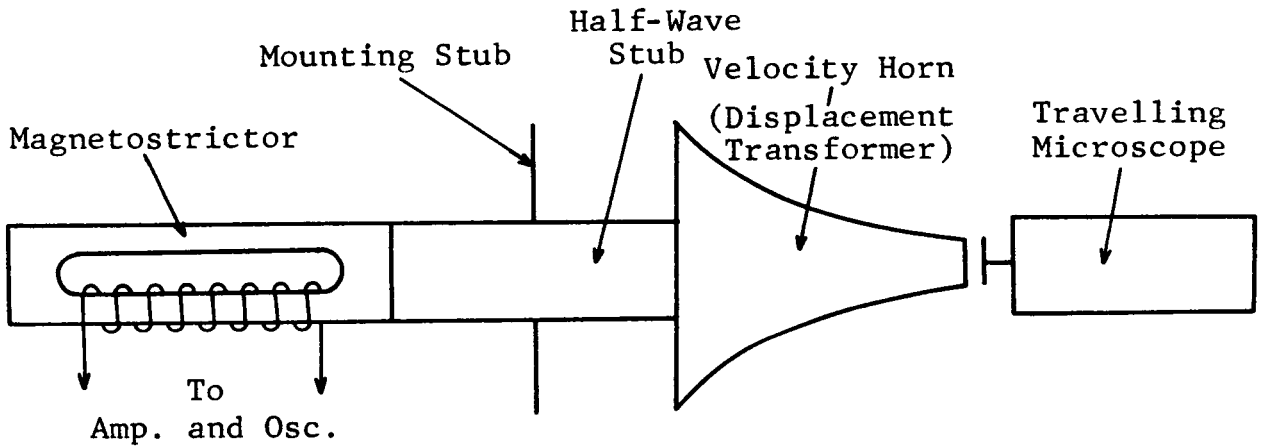

Fig. 3. Measurement System for Determining Displacements Produced by a Magnetostrictive Transducer.

produced a step-up of the transducer displacement which is proportional to the ratio of the end diameters of the velocity horn. The diameter ratio used was 6:1, which was chosen only because this exponential horn was readily available. The transducer was driven using a 1,000 watt amplifier, and, because no microphone was available during this particular test, the resulting displacements at the end of the horn were measured using a travelling microscope. From this data the sound pressure level at the end face of the horn was calculated. The displacement amplitude measured at maximum rated input power was 0.0028 in., which corresponds to a sound pressure level of 159 db at the given resonant frequency of 14.5 kc/s. This was computed by the following relationship:

$$p = \rho c v = \rho c \xi \omega$$

where p = RMS pressure (dynes/cm^2)

v = RMS particle velocity (cm/sec)

ρc = characteristic impedance of air (g/cm^{2}sec)

ξ = RMS displacement (cm)

ω = angular frequency (rad/sec)

A second magnetostrictive transducer was used at a frequency of 21 kc/s coupled to a 4 to 1 displacement transformer. A microphone was available for this test. The test included an investigation for optimum frequency, D.C. bias, microphone location, and power input into the transducer.

Under optimum operating conditions, a maximum sound pressure level of 166 db was obtained.

A third test using a magnetostrictor at a frequency of 13.6 kc/s was attempted. The results yield a sound pressure level of only 134 db, which is far below the level required for the calibration system. The results of the three tests, together with the problems and costs involved in construction of these transducers, were not encouraging, and no further consideration was given to magnetostrictive transducers.

The next high frequency generator which was investigated was a commercially available device, a Friedmann horn (Ref. 2). This device, according to its manufacturer, Macrosonics Corporation, is capable of generating sound pressure levels in the range 160 to 170 db at frequencies ranging from 21 to 39 kc/s. The Friedmann horn consists of a ceramic transducer which is mechanically coupled to a tuned pipe which vibrates in radial modes. The device was enclosed in an aluminum cylinder (Fig. 4), which was coupled to a 1/4 in. diameter tube through an exponential horn. Sound pressure levels as high as 170 db were measured in the 1/4 in. tube. However, the signal was very unstable and contained several harmonic components. A feedback system was incorporated into the electrical input to the Friedmann horn, but this did not reduce the instability in the signal. Consequently, the Friedmann horn was rejected as a possible high frequency sound generator.

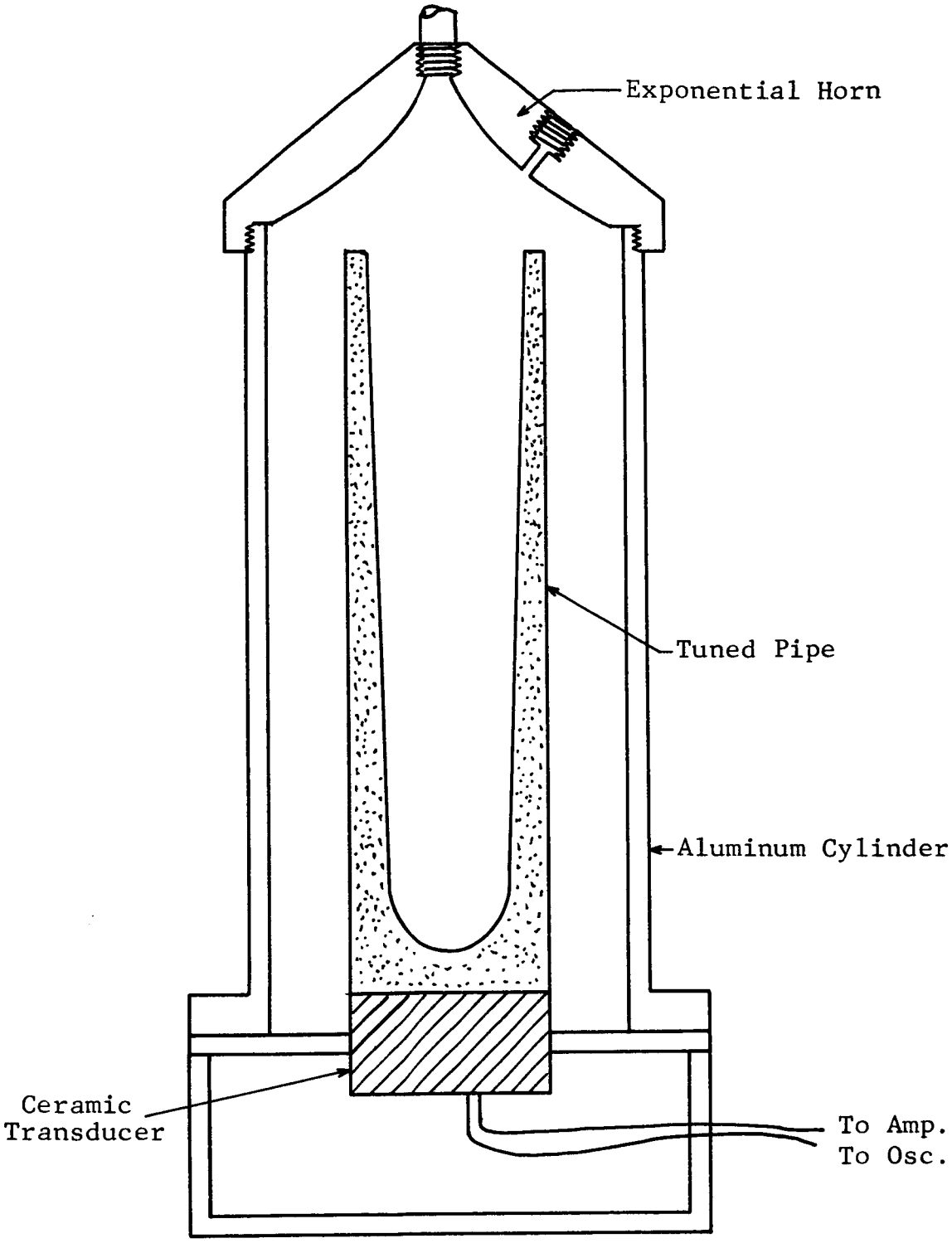

Fig. 4. Measuring System for Determining Sound Pressure Levels Generated by the Friedmann Horn.

The high frequency generator that was finally adopted for the calibration device was a St. Clair generator (Ref. 3). However, because of the complexity in the design and machining of the components for this device, other high frequency devices were first investigated; but, as previously described, all were rejected. Although several major problems were encountered in constructing and operating a St. Clair generator, it has proved to be a very effective high frequency generator, well suited to use in the calibration device.

The St. Clair generator is an electromechanical device which operates in a similar manner to the common dynamic loudspeaker. The major difference is the substitution of a rod, which is free to vibrate in a resonant mode, for the loudspeaker cone (Fig. 5). The vibrator rod is supported at its center by a 0.010 in. thick flange. The lower part of the rod has a 0.010 in. ring which is suspended in the air gap of the magnetic assembly. This ring acts as a single shorted turn secondary of a transformer (the primary is the driver coil), and is used to drive the rod at its resonant frequency. The resonant frequency of the device is dictated by the length and width of the bar. Since it was impossible to obtain a variable frequency sound source from 20,000 kc/s to 40,000 kc/s, a decision was made to construct discrete frequency generators every one-third octave from 20 kc/s to 40 kc/s. Thus four generators were constructed at frequencies of 20, 25, 30, and 40 kc/s.

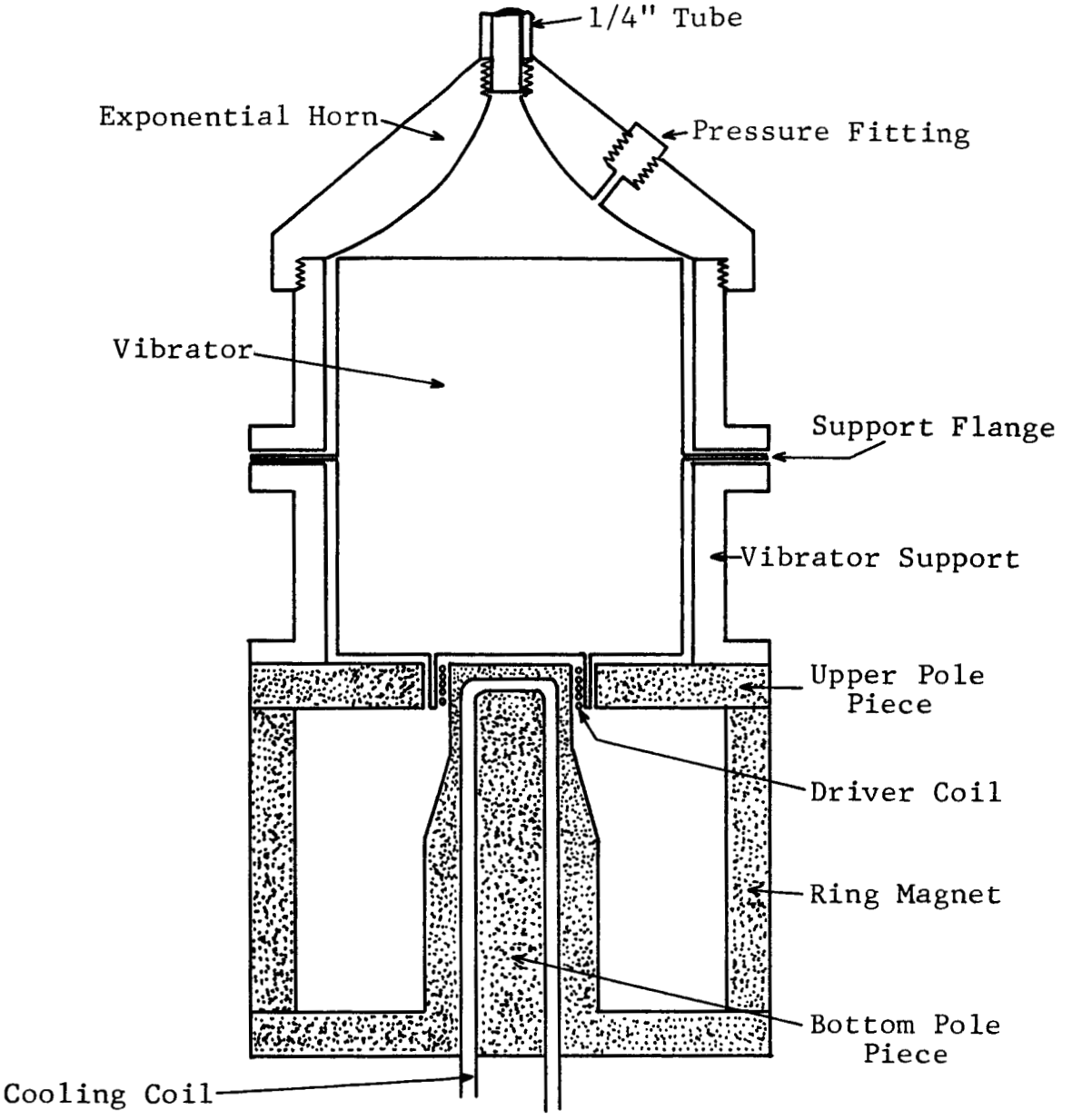

Fig. 5. St. Clair Generator.

A magnet assembly was designed which would supply the maximum flux field across the air gap. This optimized magnetic system was not realized since commercially available magnets could not be purchased having the exact dimensions required. The time and cost involved in obtaining customized ring magnets could not be accommodated in this program. Thus the magnetic assembly was modified slightly to accommodate commercially available ring magnets with a minimum of optimized flux density loss.

The ring magnets chosen for the St. Clair generators were made of Alnico V and each had to be fabricated from two ring magnets. Problems were encountered in bonding the magnets together and also in the eloxing of the mounting holes which then had to be filled with a softer material to simplify machining processes. The major difficulty in the assembly of these generators was encountered in the mounting of the vibrating rod. If the flange on the vibrator was clamped too tightly, the sound output was decreased 40 to 50 db below maximum output level. Therefore, the mounting of the rods and the clamping of the flanges became critical steps in the construction process. Whenever the generator was damaged, the complete assembly had to be de-magnetized, disassembled, repaired, re-assembled, and finally re-magnetized. This was costly and time-consuming although, as additional generators were constructed, the problems encountered in the earlier generators were avoided.

An aluminum housing was constructed for the generator. This was fitted with an exponential horn which could then be attached to the acoustic cavity in the calibrator device. All the St. Clair generators are capable of being operated under reduced ambient pressures.

The vibrator rod has an extremely high Q factor, having a band-width of one or two cycles, which makes manual tuning of the system virtually impossible. Thus a capacitance pickup was mounted on the center pole piece of the magnet assembly which could be used as a feedback pickup. This feedback pickup was fed into a pre-amplifier (Fig. 6) and then to an amplifier. A phase-shift network was constructed into the feedback system to enable the generator to be self-oscillatory (Fig. 7). This proved highly successful for all four generators, producing sound pressure levels in the range 168 to 174 db.

During one test, without any feedback system, the 20 kc/s and 40 kc/s generators were operated at their harmonic frequencies to determine the sound pressure level produced at these frequencies (Fig. 8). Again, the problem of maintaining a tuned system was experienced because the narrow band-width made continuous operation difficult. A paralleled 'T' filter was designed which would allow the feedback system to be utilized to operate the generators at their harmonics (Fig. 9). A preliminary test of this system indicates that it will function as designed. However, time did not permit the required extensive testing of the system.

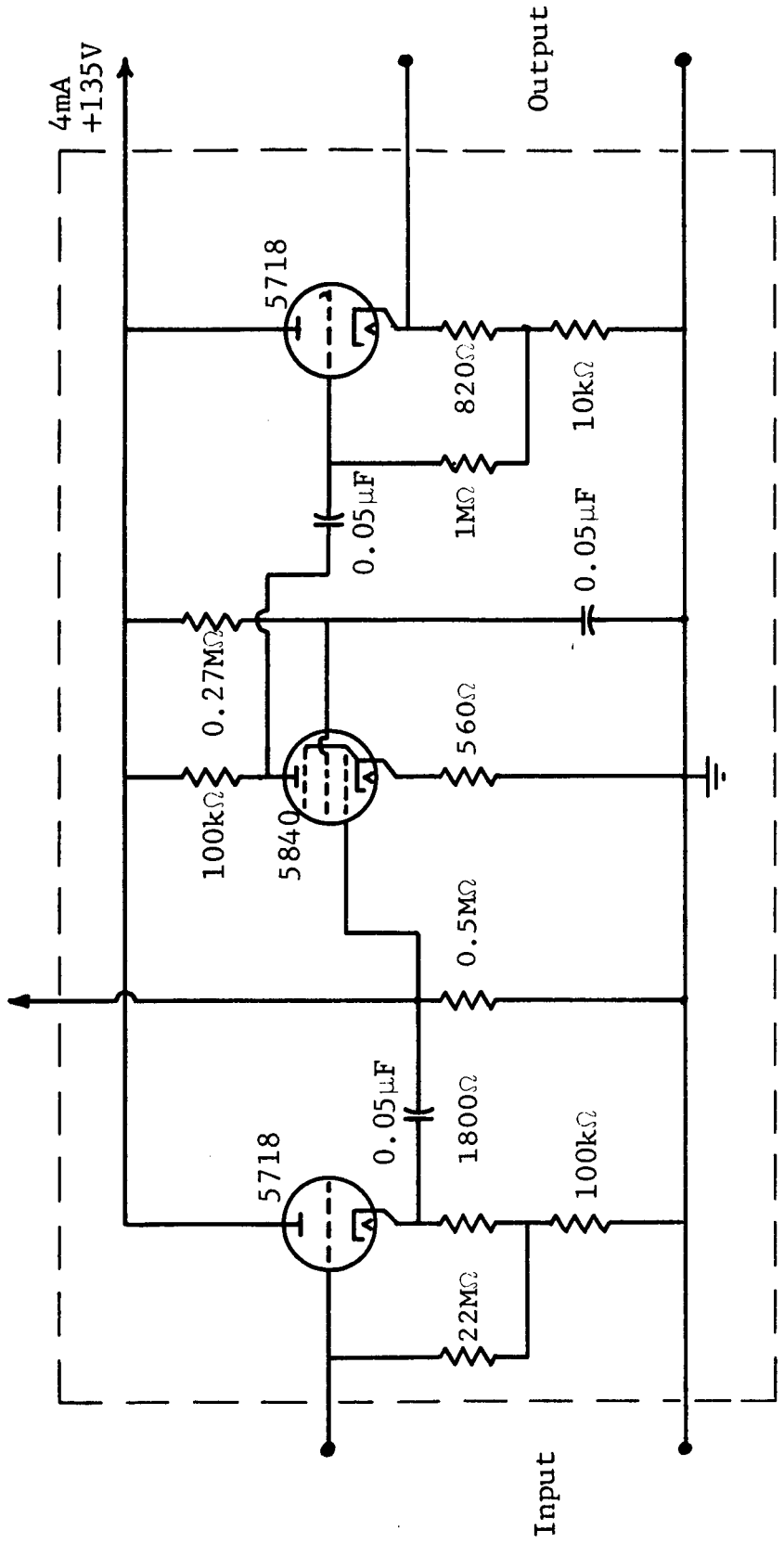

Fig. 6. Circuit Diagram for Pre-amplifier Used in Feedback System for St. Clair Generator.

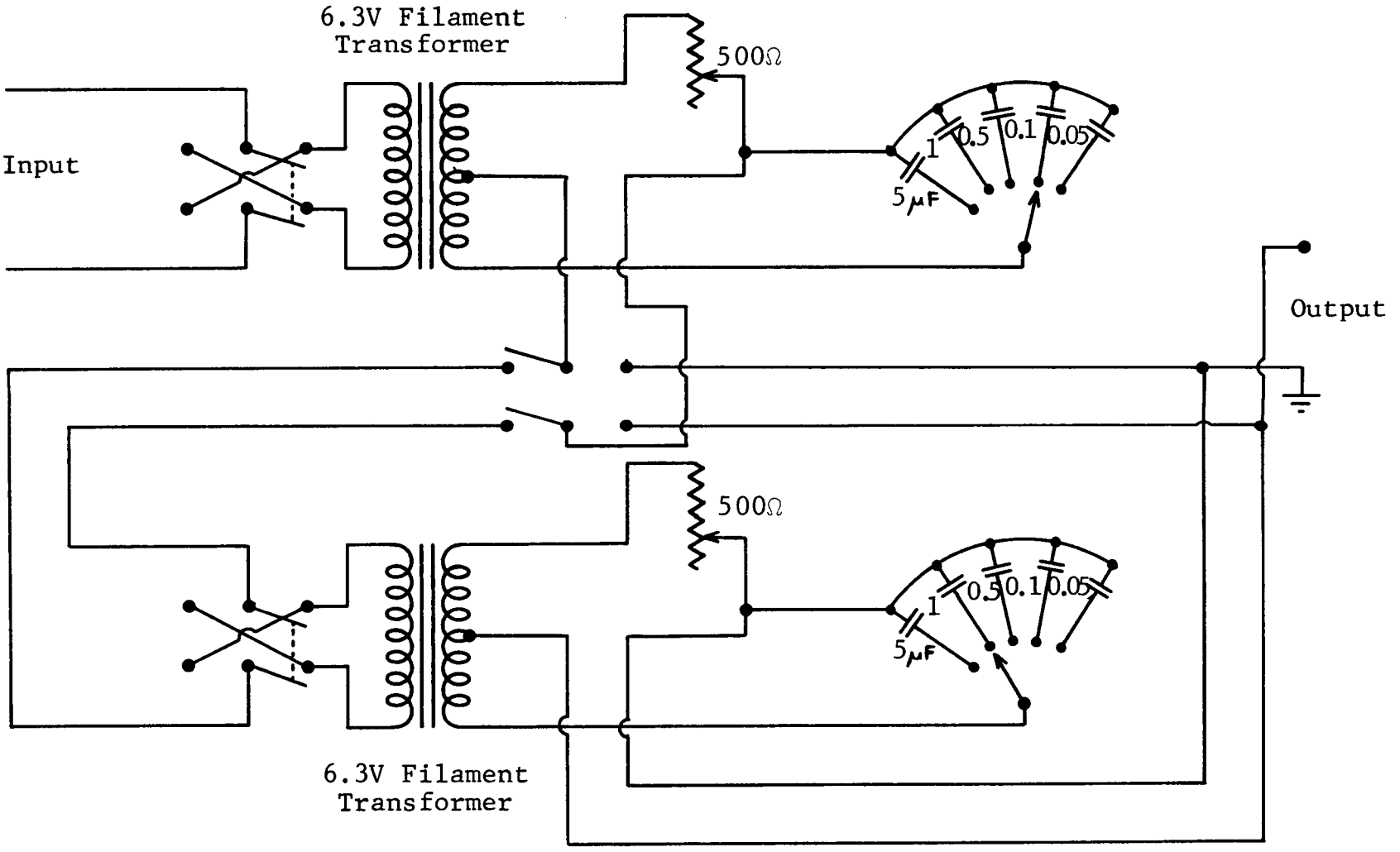

Fig. 7. Circuit Diagram for Phase Shifter Used in Feedback System for St. Clair Generator.

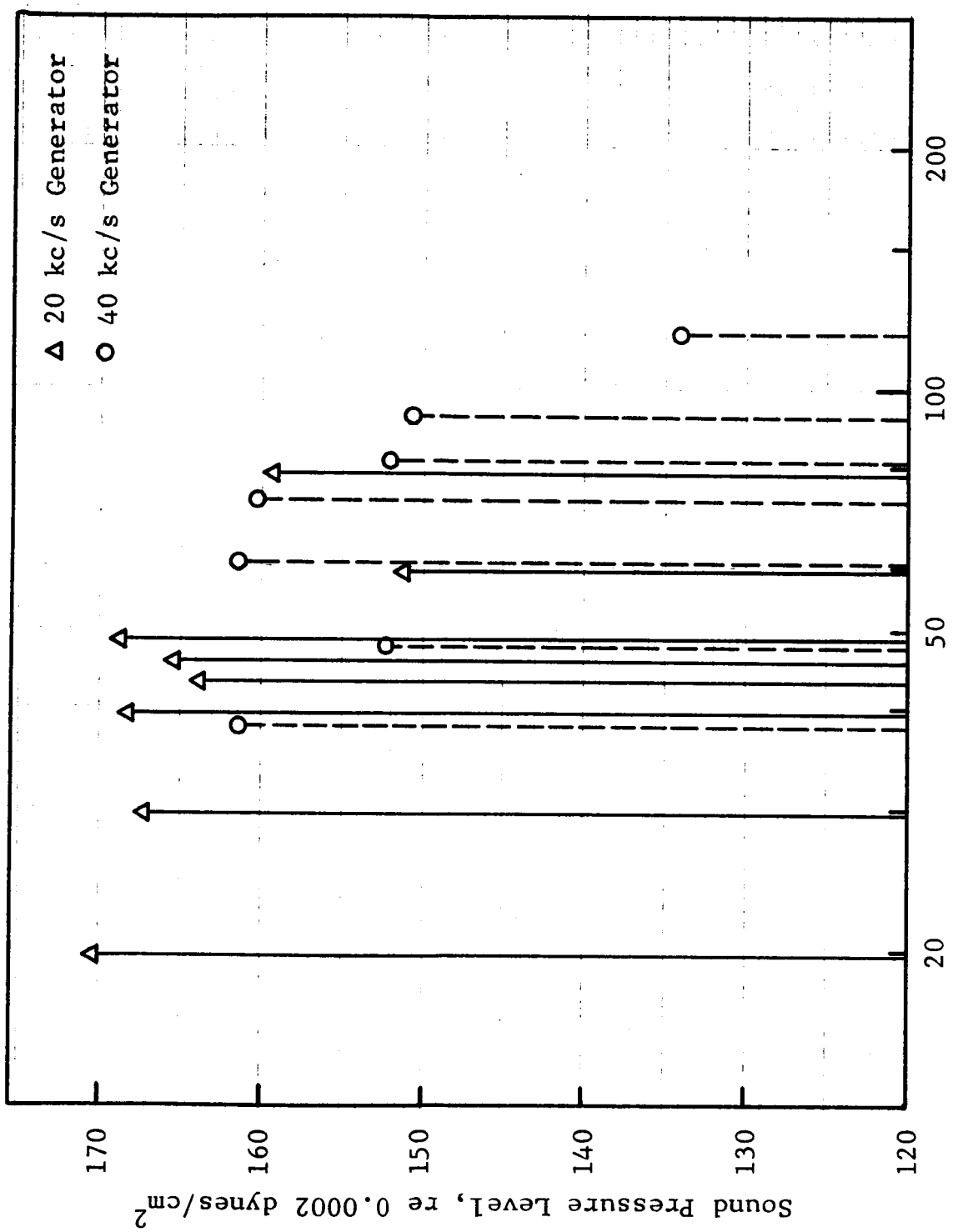

Fig. 8. Sound Pressure Levels Generated by St. Clair Devices Operated at Their Harmonic Frequencies.

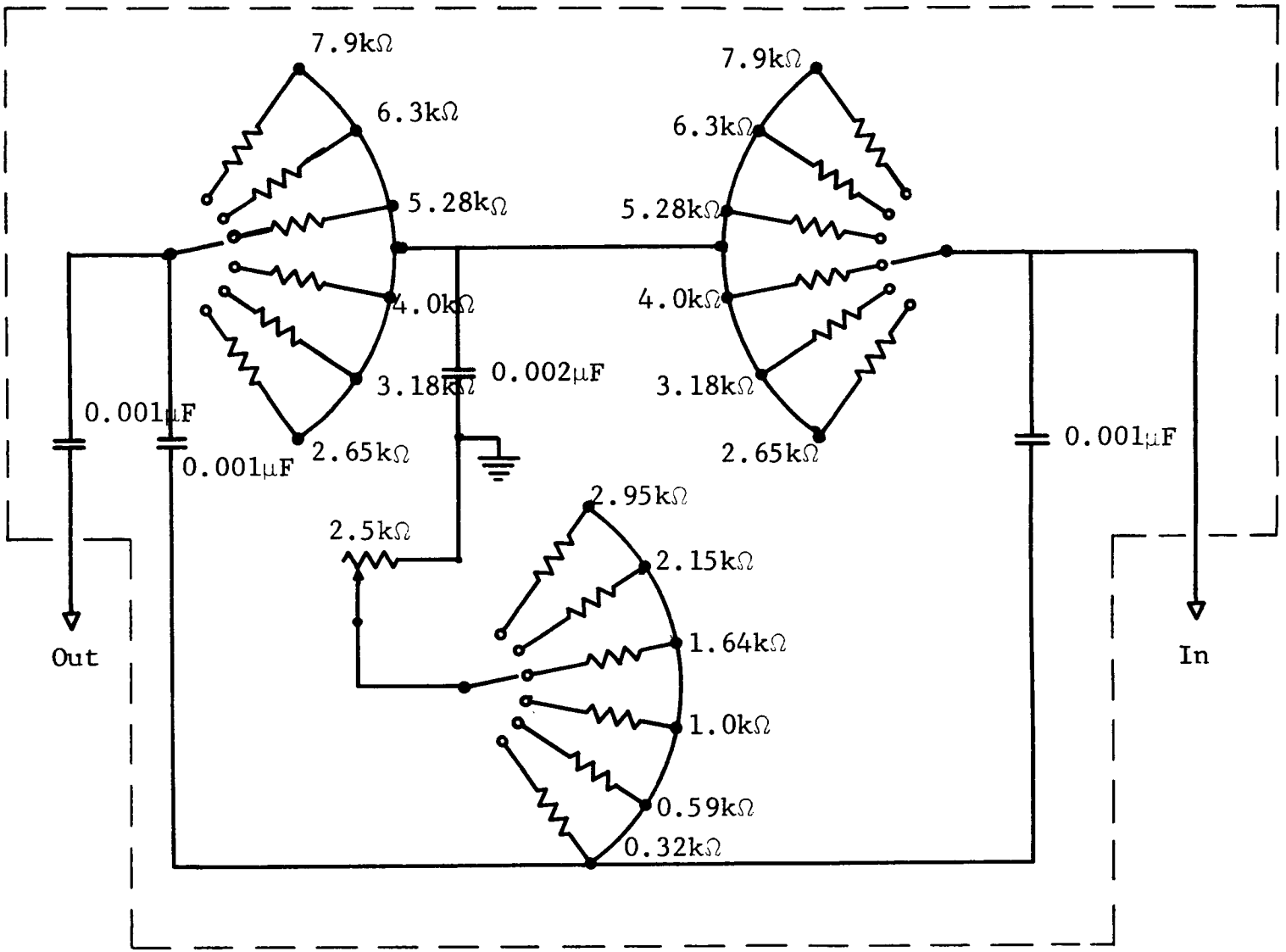

Fig. 9. Circuit Diagram of Parallel T Filter Used in Feedback System for Harmonic Operation of St. Clair Generators.

Acoustic Fields in the Calibration Cavity

The cavity into which unknown transducers will be introduced in the complete calibration system has an internal diameter of 1/4 in. The effective length of the cavity is determined by the distance from the end of the tube, terminating at the coupling unit of the horn-drivers or the exponential horn of the St. Clair generators, to the location of the unknown transducer. Mechanical considerations in the final design of the system dictate this length to be approximately 2 in. It is desirable to make this length as short as possible to reduce the energy dissipation at high frequencies which would result in reduced sound pressure levels. In order that advantage can be taken of longitudinal resonances in the cavity, a degree of tuning is provided because the cavity is constructed from telescopic sections. This also enables the sound generators to be removed from the calibration system, leaving the portion of the cavity containing the unknown transducer and optical windows in situ in the interferometer section. If an increased sound pressure level is required in the cavity at a given frequency of operation, this may possibly be achieved by varying the effective length of the cavity through adjustment of the telescopic sections.

It can be seen in Fig. 2, from the envelope of the sound pressure levels that could be obtained using any of the horn-drivers, that beyond a frequency of approximately 16 kc/s

there is considerable reduction in the sound pressure level. This indicated that sound cancellation effects, due to cross-mode production in the 1/4 in. diameter tube, may have occurred in this frequency region. Cross-mode production is normally accepted to occur at frequencies above a critical frequency whose wavelength is between three and four times the tube diameter. For a 1/4 in. tube the critical frequency would occur in the region between 13 and 18 kc/s. Below these frequencies acoustic plane waves would be produced in the cavity. Thus the sound pressure level would be constant over any cross-section through the cavity. Therefore, the pressure level sampled by the interferometer will be identical to that at the face of the transducer requiring calibration. This also demands that the optical sampling be performed immediately in front of the transducer. If cross-modes occur so that transverse sound pressure level gradients and phase variations exist in the cross-section of the cavity immediately in front of the transducer requiring calibration, the following effects will occur. First, pressure cancellations will reduce the transducer response from the level that would be obtained under plane wave conditions. Second, the interferometer will, similarly, respond to density fluctuations averaged over the optical path across the cavity. Consequently, calibration of transducers under these conditions becomes subject to error. It is beyond the scope of this program to devise correction

procedures for calibrations under these conditions. Consequently, it is essential to establish the frequency at which these effects occur and if possible to delay the onset of cross-mode production.

An experiment was devised to explore the sound field in a cross-section of the 1/4 in. diameter tube. A mechanical traversing system was constructed so that a microphone would accurately measure the sound field across the end of the tube. This was accomplished by constructing a thin metal plate in which a 0.015 in. hole was drilled. This plate was interposed between the tube end and the microphone and by traversing this plate across the tube diameter the sound pressure level was sampled at positions across the tube.

The sound pressure level was determined across two mutually perpendicular diameters at the end of the 1/4 in. tube at a given frequency. In Fig. 10, the range of the maximum variation in the sound pressure levels in the cross-section of the tube is shown. The data indicates that cross-mode effects are present even at frequencies below 16 kc/s, but the effects are small in this region. Above 20 kc/s, the effects are very pronounced, and the following steps were taken to delay the onset of cross-mode production. Since the velocity of sound in helium gas is approximately three times greater than that in air, cross-mode production in the cavity filled with helium should not occur below frequencies in the approximate range 40 to 55 kc/s. The previous experiments were

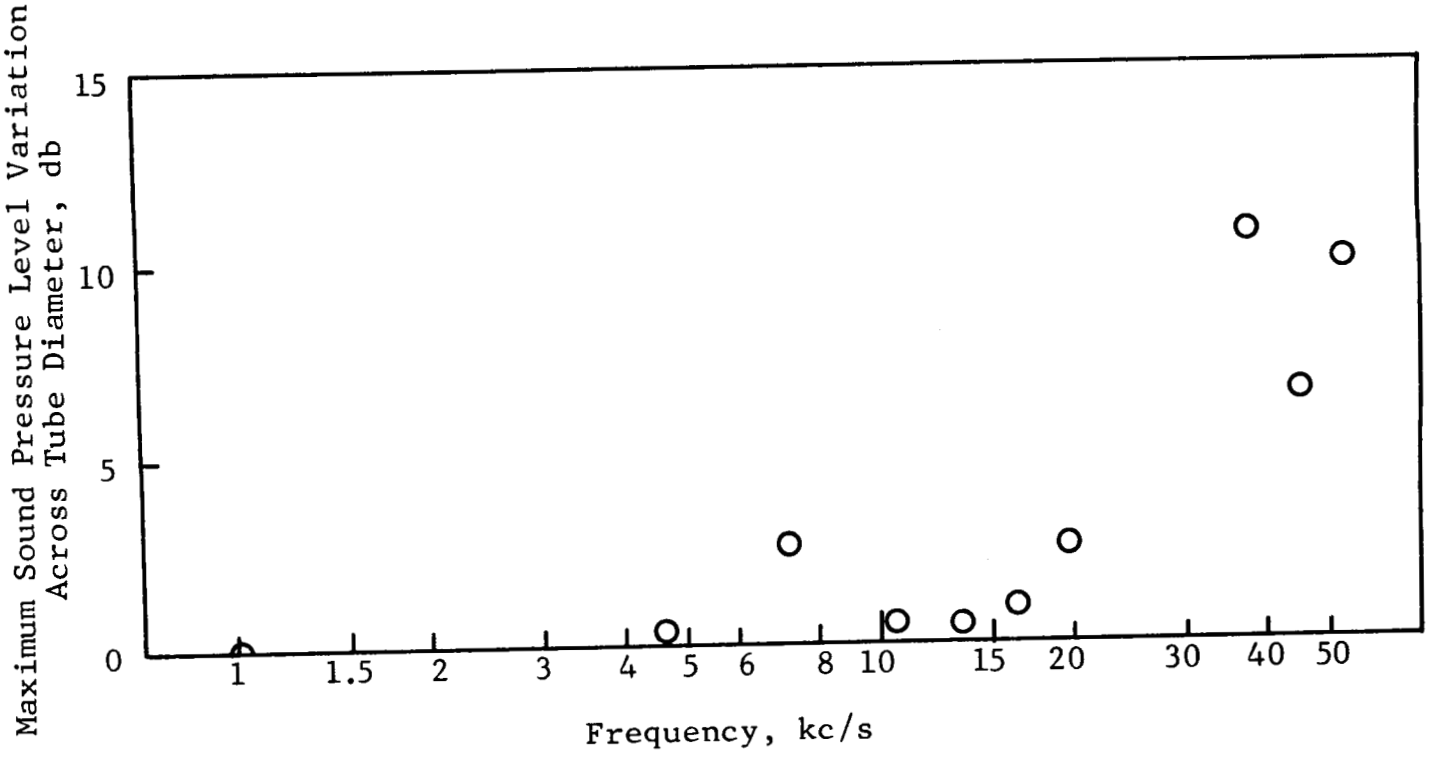

Fig. 10. Cross-Mode Effects in 1/4 in. Diameter Tube.

repeated with the 1/4 in. tube filled with helium. It was found that the variations in sound pressure level across the tube were minimal and at a frequency of 60 kc/s were only $\pm$ 1 db. Consequently, it is necessary that when accurate calibrations are required, helium must be substituted for air at frequencies above 16 kc/s, i.e., whenever the St. Clair generators are used in the system.

It may be noted that these experiments were conducted at low sound pressure levels using a horn-driver unit. When helium was substituted for air, the generated sound pressure levels were reduced, as shown in Fig. 11. It was not established whether the same effect would be observed using the St. Clair generator devices.

In conclusion, it is anticipated that successful calibration can be achieved using this cavity filled with air to 16 kc/s and to the required 40 kc/s when filled with helium. The first conclusion is supported by calibration tests reported in Section V.

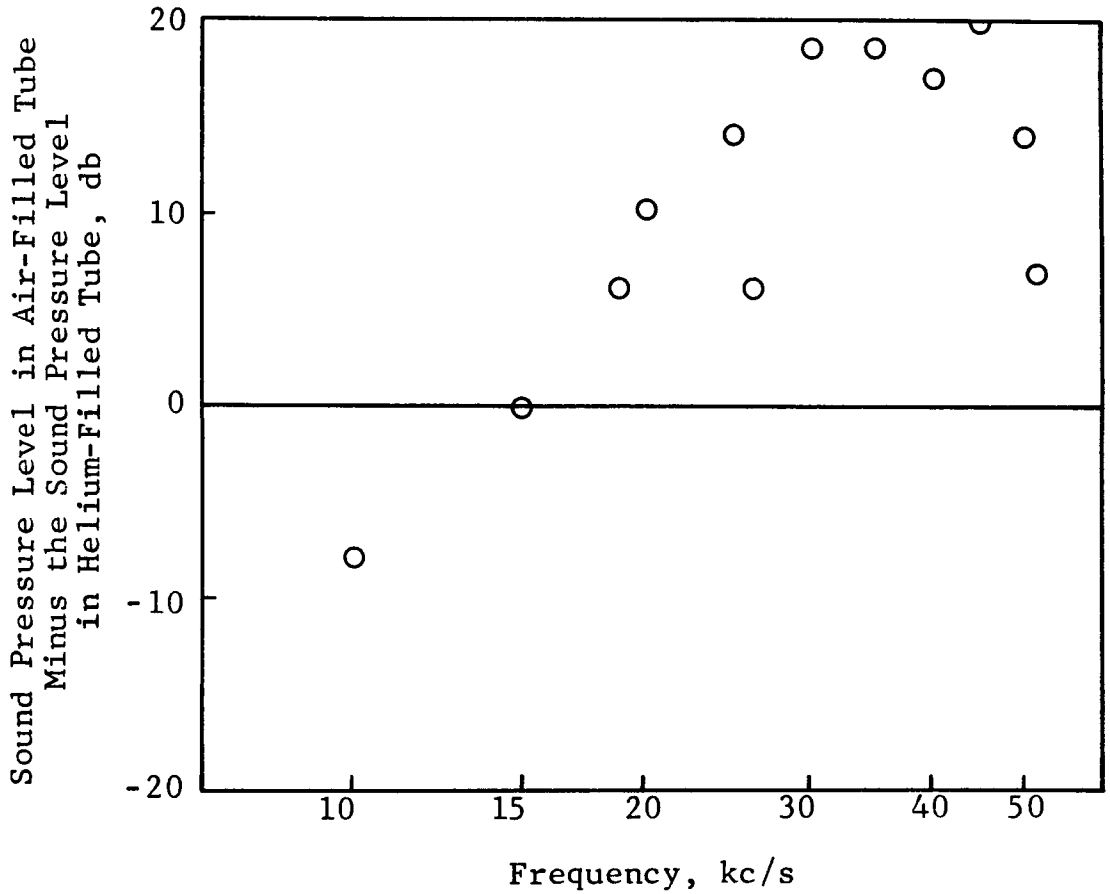

Fig. 11. Difference in Sound Pressure Levels in 1/4 in. Diameter Tube Filled with Air and Helium.

III. OPTICAL SYSTEM

Using one of the acoustic generators described in the previous chapter, an acoustic signal may be produced in the resonance tube containing the transducer requiring calibration. Determination of the sound pressure level of this acoustic signal is accomplished through measurement of the associated density changes in the air medium using an optical interferometer. The choice of interferometer was between the multiple-beam type of interferometer such as the Fabry-Perot and the double-beam interferometer such as the Michelson.

The interferometer is required to measure a wide range of density changes corresponding to peak fringe order changes between 0.07 and 2.3 for a double pass across the diameter of the given acoustic cavity. This range of fringe excursions indicates that the double-beam type of interferometer would be ideal; consequently, the Michelson interferometer was chosen for its simplicity of construction and ease of operation. The light source was chosen to be a helium neon laser system.

The optical-acoustical assembly is shown in Figs. 12, 13, 14, and 15. Figures 13 and 14 are 1/4 size, and Fig. 15 of the interferometer is 1/2 size. All components were mounted on an aluminum base plate 1 x 14 x 30 in., chosen for its large mass and stiffness. The interferometer is suspended from an overhead yoke to provide the necessary clearances, and to isolate the interferometer base from flexure in the large

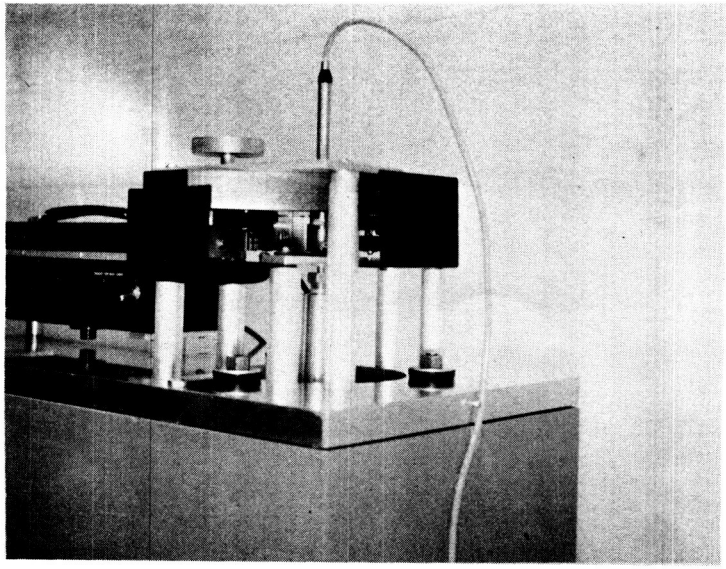

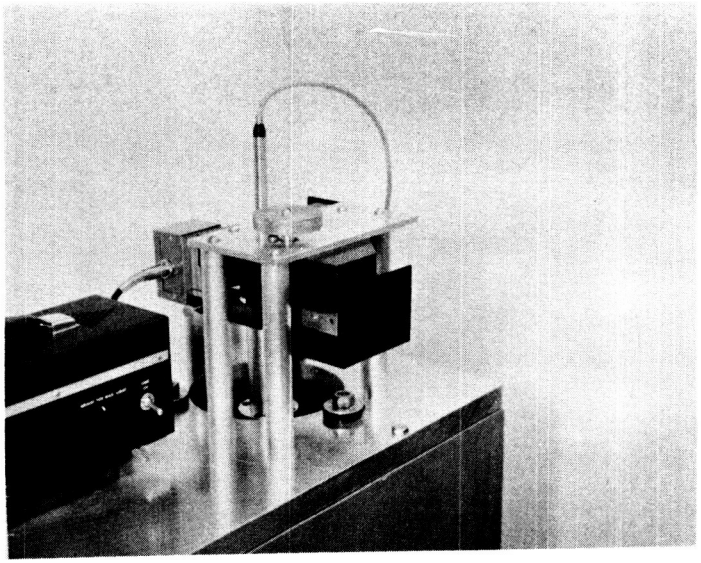

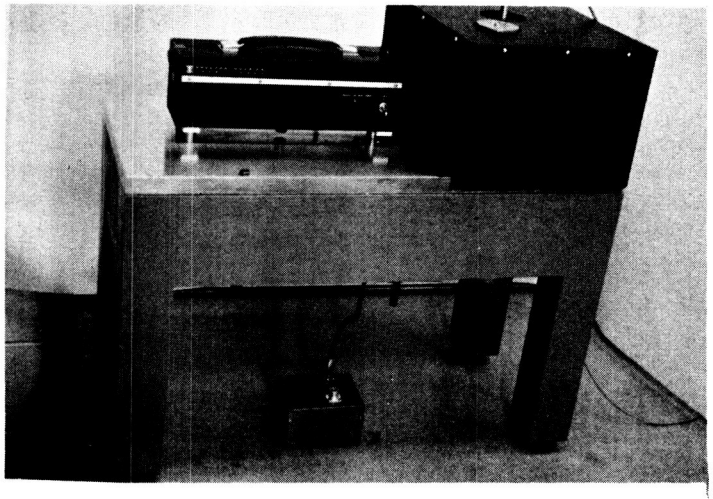

Fig. 12. Views of the Interferometer and the Complete Calibration Device Assembly.

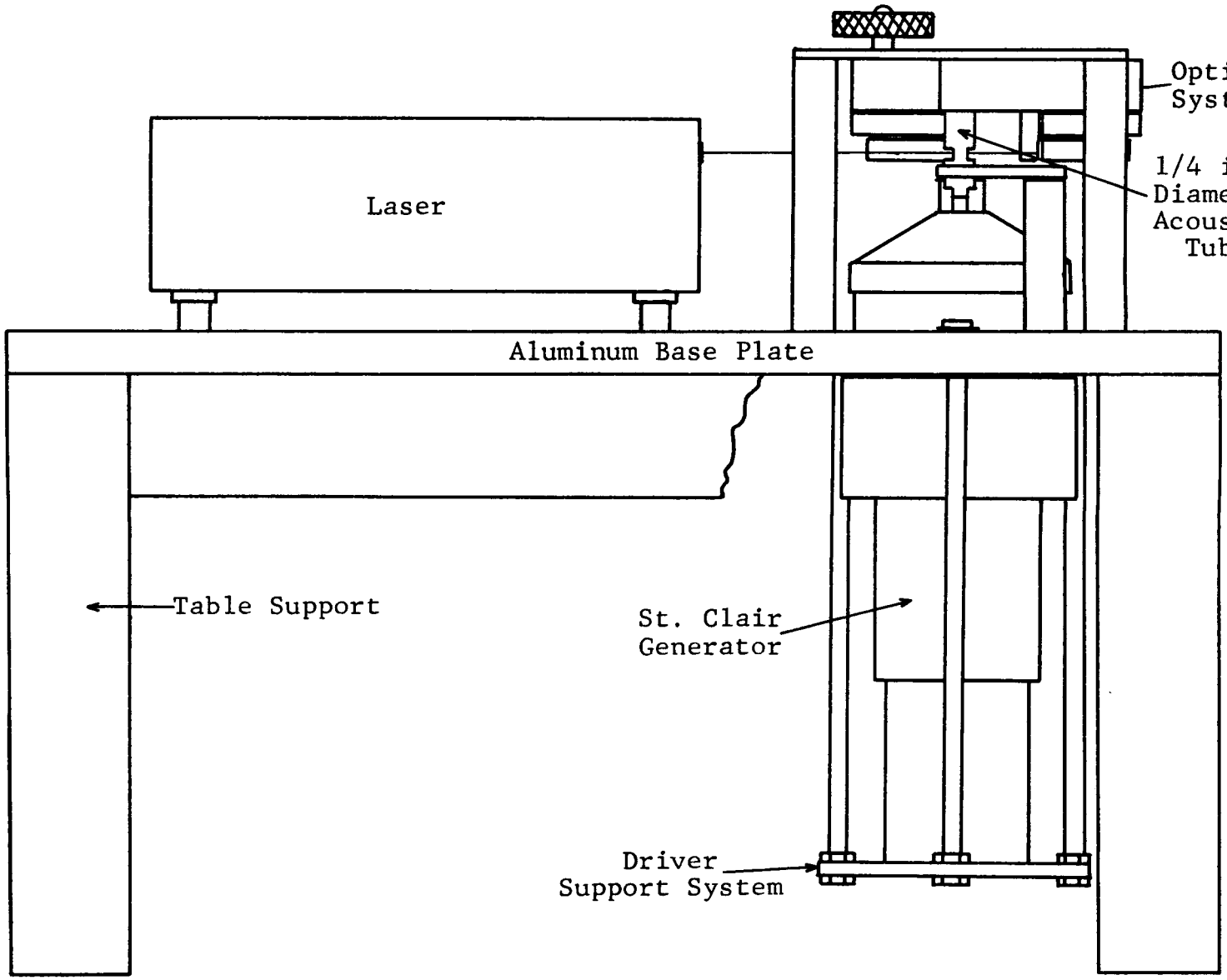

Fig. 13. Calibration Device Assembly, Front View with Protective Cover and Guard Plate Removed.

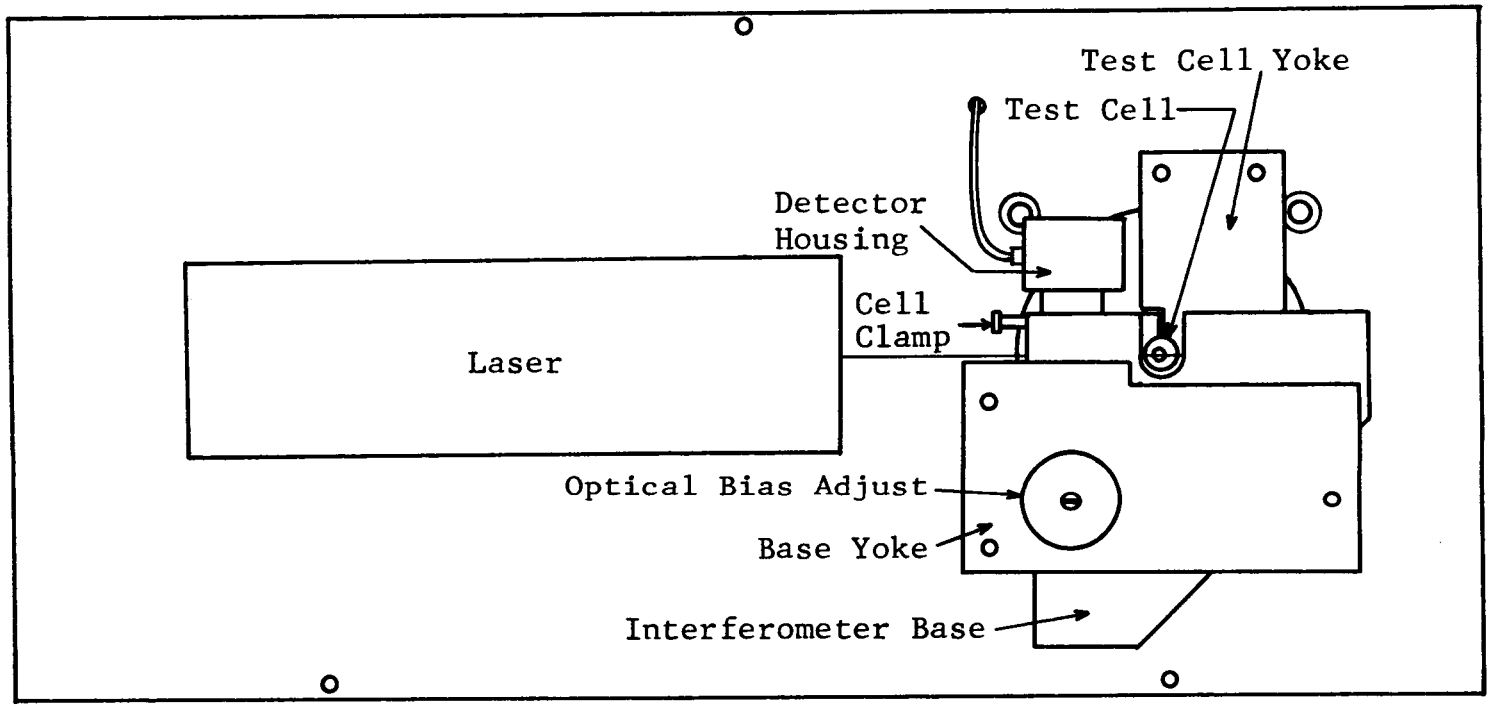

Fig. 14. Calibration Device Assembly, Top View with Protective Cover and Guard Plate Removed.

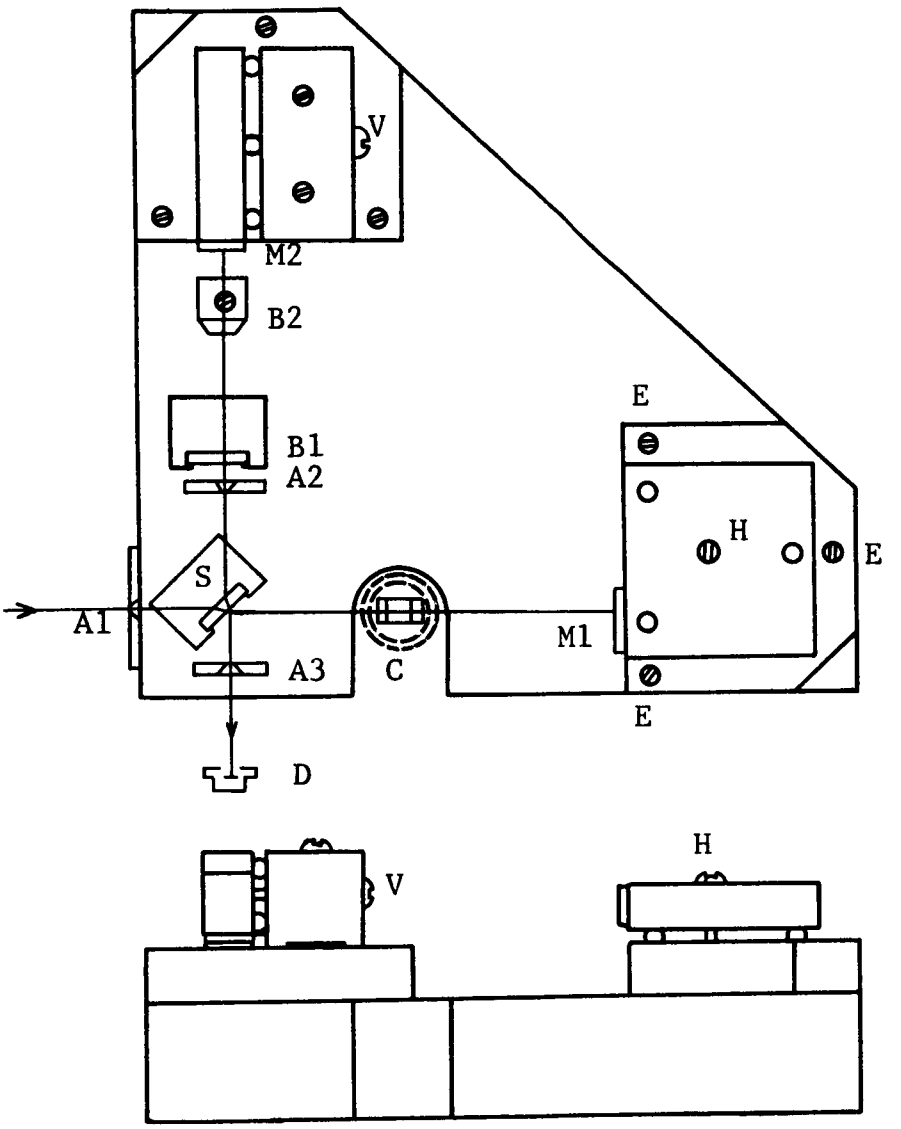

Fig. 15. Detailed Assembly of Optical Interferometer, Viewed from the Underside.

base plate. A guard plate is located directly beneath the interferometer to protect it from damage during the process of interchanging the acoustic generators, etc. The test cell is clamped in a second yoke in order to locate the cell with respect to the interferometer without direct attachment to the interferometer base. This yoke is mounted in rubber grommets on widely spaced centers for vibration isolation with minimum angular displacements. The cell will remain clamped while drivers are interchanged. All components are mounted above the base plate on suitably tall columns in order to prevent accumulation of heat from the laser beneath the base plate and consequent expansion of the interferometer base. The front leg of the laser is slot-mounted for differential expansion between the laser housing and base plate. The acoustical drivers are suspended through a hole in the base plate by means of three grommet-mounted threaded 1/2 in. rods and a platform.

The optical paths in the interferometer are shown in Fig. 15, as seen from the underside in the operating position. The lower beam enters the interferometer through a 1 mm. aperture A1. The beam splitter S transmits approximately 91 percent and reflects 9 percent of the incident beam, which is plane-polarized perpendicular to the plane of incidence. The transmitted portion traverses the acoustic cell C, is reflected back through the cell, and finally 9 percent is reflected by the beam splitter to the detector D. The second beam traverses

a similar path but makes an additional two transmissions through the beam splitter. The intensity of this beam at the detector, therefore, is slightly less than that of the first beam. Consequently, complete extinction of the two interfering beams is not possible. The final intensity of each of the beams at the detector is approximately 5.5 percent of the incident intensity. The total intensity on the detector, then, varies from near extinction to 22 percent of the incident beam according to the path difference between the two beams of the interferometer.

The laser beam is 1.6 mm. in diameter at the laser semi-reflecting mirror. The diameter is reduced to 1 mm. by the defining aperture A1, rigidly pinned to the interferometer base. Aperture A2 rejects the unwanted front reflection from the beam splitter, and also weak multiple reflections. Aperture A3 performs a similar function for the beam from M1, as well as eliminating multiply reflected components from both beams upon reunion at S. The glass plates B1 and B2 approximately compensate for the change in total optical path length introduced by the cell windows. Rotation of compensator B2 by means of a knurled knob through a small angle near normal incidence provides a means of adjustment of the mean phase difference, the optical bias point. Division of B into two plates keeps the number of glass-air interfaces equal for minimum intensity at extinction, and also permits use of a thinner plate at B2 to make the angular adjustment less critical to the touch.

The mirrors are set to reflect slightly away from normal incidence in order not to return light through A1 to the laser exit mirror. Since this mirror is accurately perpendicular to the beam, it would form a set of satellite interferometers with M1 and M2 resulting in complexities of adjustment and interpretation. The large component returned by M1 through S falls horizontally adjacent to the 1 mm. aperture A1. A weaker beam from M2 is also intercepted at exactly the same point. The aperture A2 is oversize in order to transmit both the incident and reflected beams of M2. A3 is slightly over size.

The pressure cell C and the plate B1 are mounted not quite perpendicular to the traversing beams in order to deviate secondary reflections away from A3.

Mirror M1 can be tilted very slightly about a horizontal axis behind and below its center by the screw H, which bends the plate to which M1 is cemented. This plate is mounted to a pedestal by means of three intervening steel balls in cylindrical sockets deformed by pressure into spherical contacts for smooth angular displacement of the mirror. A similar fine adjustment of M2 about a vertical axis is provided by V. The deformable plates are thick and short so that the forces required to tilt the mirror significantly are large in comparison to extraneous vibrational forces introduced through the base plate.

IV. THEORY AND OPERATION OF CALIBRATION DEVICE

Optical Interferometer Theory

For the Michelson type of interferometer, the fringe system is such that

$$\sum_1 \mu d - \sum_2 \mu d = m\lambda \qquad (1)$$

is the condition for the production of bright fringes, i.e., both optical beams combine in phase. In this expression, $\sum_1 \mu d$ and $\sum_2 \mu d$ are the total optical path lengths of beams 1 and 2 respectively, λ is the wavelength of the electromagnetic radiation, and m is the fringe order. The only variable in the proposed system is the refractive index of the gas in the acoustic cavity. Refractive indices and distances through which the two beams travel remain constant elsewhere. Consequently, we may rewrite Eq. (1) in the form

$$\Delta\mu \cdot d = \Delta m\lambda \qquad (2)$$

where $\Delta\mu$ represents a change in refractive index in the gas in the acoustic cavity, d the total optical path length in the cavity, and Δm the change in fringe order associated with the refractive index change $\Delta\mu$.

The refractive index of a gas may be related to the density of the gas by the Gladstone-Dale constant (Ref. 4, p. 7)

$$\frac{\mu - 1}{\rho} = \text{constant} = r \qquad (3)$$

which is a good approximation for gases to the Lorenz-Lorentz function (Ref. 4, p. 8)

$$\frac{1.5\ (\mu^2 - 1)}{(\mu^2 + 2)\rho} \tag{4}$$

If we allow μ to change by an increment $\Delta\mu$ and allow ρ to change correspondingly by an increment $\Delta\rho$ then from Eq. (3)

$$\frac{\mu + \Delta\mu - 1}{\rho + \Delta\rho} = r \tag{5}$$

or

$$\Delta\mu = r\Delta\rho \tag{6}$$

Equation (6) enables us to relate changes in refractive index with changes in density. Now we can combine Eqs. (2) and (6) to obtain the relationship between the change in the density of the gas in the acoustic cavity and the corresponding change in the fringe order associated with the density change. Thus

$$r\Delta\rho d = \Delta m \cdot \lambda \tag{7}$$

We must now relate the change of density of a gas with change of pressure.

For a gas, assuming adiabatic conditions, we have

$$p = k\rho^{\gamma} \tag{8}$$

Thus incremental changes in pressure and density are related by

$$\frac{\Delta p}{p} = \gamma \frac{\Delta\rho}{\rho} \tag{9}$$

Combining Eqs. (7) and (9) we have

$$r \frac{\Delta p}{p} \frac{\rho d}{\gamma \lambda} = \Delta m \qquad (10)$$

This equation is the basis for the determination of pressure change by measuring the associated fringe order change in an interferometric device. However, the value of the constant r must first be evaluated. This may be achieved, by returning to Eq. (3), from knowledge of the refractive index and density of the given medium under some standard conditions. We chose the medium to be air and the conditions to be 15°C and 760 mm. of mercury pressure.

The refractive index of air under these conditions can be calculated from the Cauchy dispersion formula (Ref. 5)

$$(\mu-1)\ 10^7 = 2726.43 + \frac{12.288}{\lambda^2 \times 10^{-8}} + \frac{0.3555}{\lambda^4 \times 10^{-16}} \qquad (11)$$

Using the value of λ = 6328 A° for the helium neon gas laser wavelength, we find

$$(\mu-1) = 2.759 \times 10^{-4} \qquad (12)$$

Reference 5 gives the density of air at 0°C and 760 mm. of mercury pressure equal to 1.2929×10^{-3} gm/cm^3. Corrected to 15°C its value is 1.2256×10^{-3} gm/cm^3.

Thus the value of r, using the above values for λ and ρ is 0.22511. The value of d, the total optical path length in the acoustic cavity, is equal to twice the distance between

the inner surfaces of the windows in the cavity (because the optical beam traverses the cavity twice). The value for d is 1.3208 cm. for the given system.

Using the following values for the parameters of Eq. (10)

$r = 0.22511$

$p = 1.01325 \times 10^{6}$ dynes/cm^2 (760 mm. of mercury)

$\rho = 1.2256 \times 10^{-3}$ gm/cm^3

$\gamma = 1.403$

$\lambda = 6.328 \times 10^{-5}$ cm.

$d = 1.3208$ cm.

we have

$$4.0509 \times 10^{-6} \Delta p = \Delta m \qquad (13)$$

This equation is valid for air behaving in an adiabatic manner and forms the basis for the measurement of pressure by the measurement of the associated fringe order change in the given interferometric device. In practice, Eq. (13) is utilized in the following manner.

An applied acoustic pressure of R.M.S. amplitude p dynes/cm^2 has a peak to peak value of $2\sqrt{2}$ p if the signal is sinusoidal. This peak to peak pressure amplitude corresponds to the value of Δp in Eq. (13) because, in the proposed method of interferometric signal interpretation, it is the peak to peak fringe order change which can conveniently be determined. Thus, rewriting Eq. (13), we have

$$1.1456 \times 10^{-5}\ p = \Delta m \qquad (14)$$

where Δm is now considered to be the peak to peak fringe order change and p is the R.M.S. pressure amplitude of the applied acoustic signal. The value of this pressure as a sound pressure level is

$$P = 20 \log_{10} \left[p/2 \times 10^{-4} \right] \text{ db} \qquad (15)$$

Figure 16 illustrates the relationship between the peak to peak fringe order change Δm and the sound pressure level P db. This curve is obtained using Eqs. (14) and (15).

If the interferometer is operated with the air medium in the cavity at pressures other than atmospheric, Eqs. (13) and (14) and consequently the curve in Fig. 16 are still valid. However, if the air medium is replaced by another gas such as helium, these equations must be modified using different values for the parameters of Eq. (10).

Reference 5 gives the value of $(\mu-1)$ for helium (under atmospheric conditions) as 3.6×10^{-5} for the sodium D line. Literature searches have not revealed a value corresponding to the helium-neon gas laser wavelength. Using this alternative value an error of 1 or 2 percent is anticipated. Reference 5 gives a value of 1.66 for γ for helium and thus re-evaluating Eq. (10) for helium gives

$$1.263 \times 10^{-6}\ p = \Delta m \qquad (16)$$

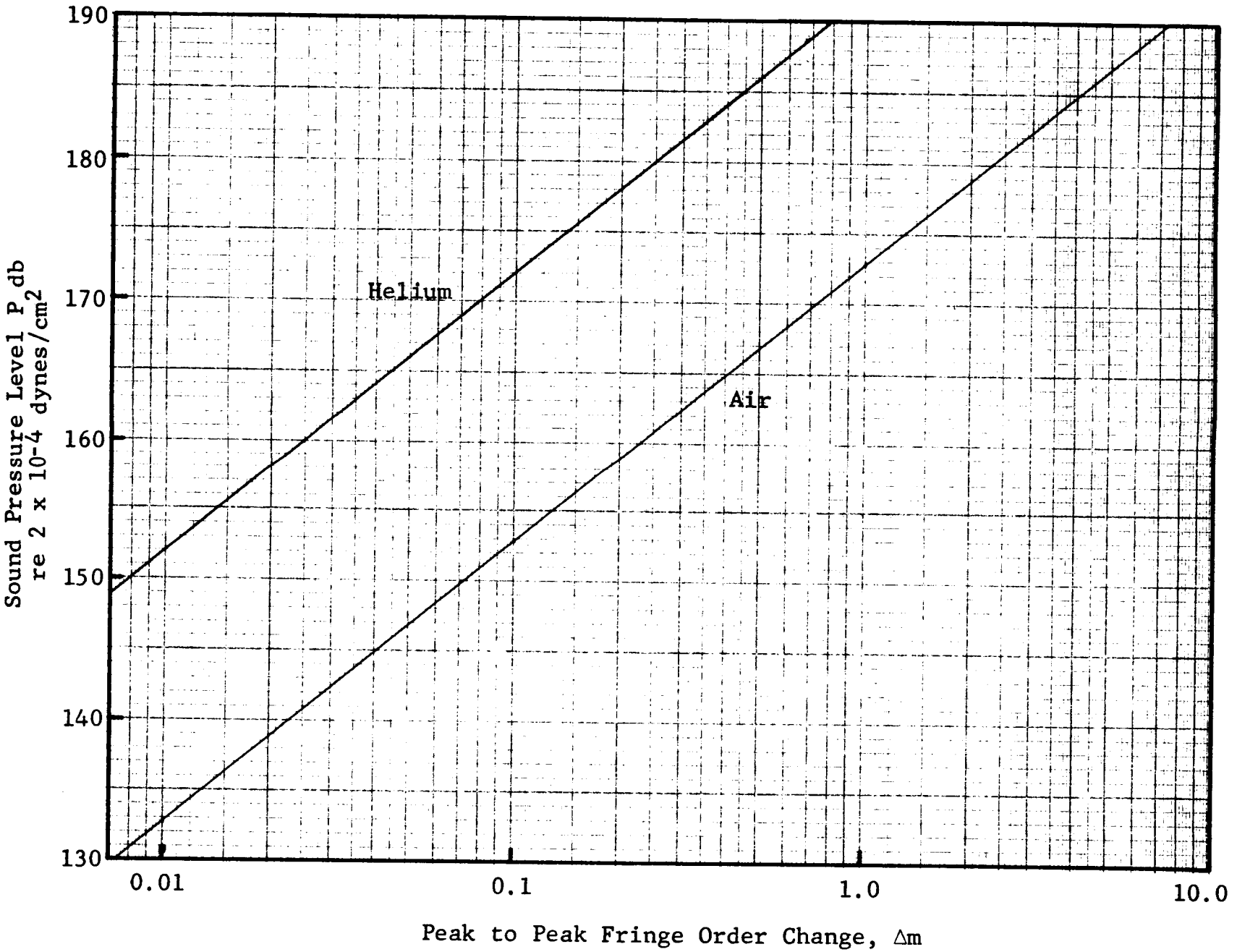

Fig. 16. Relation Between the Sound Pressure Level in the Given Cavity and the Associated Peak to Peak Fringe Order Change, Δm.

Figure 16 illustrates the relationship between the peak to peak fringe order change Δm and the sound pressure level P db for helium using Eqs. (15) and (16).

Calibration Technique

Michelson interferometric fringes have a cosine squared intensity distribution as shown in Fig. 17. A portion of the intensity is shown for a typical series of fringes of order --- m, m + 1, --- where m is an integer. In the suggested use of the calibration device, an optical compensator is provided so that initially, before any acoustic signal is applied to the acoustic cavity, the photodiode detector observes the fringe system at the point X whose order m_x is such that $m_x + 1/4$ is an integer, n. The point X is chosen for convenience in signal interpretation, though the compensator enables any point on the fringe system to be obtained. At X, the observed intensity is the mean of the maximum and the minimum intensities of the fringes, since the point X lies exactly one-quarter of an order from an intensity maximum and one-quarter of an order from an intensity minimum. The reasons for this choice of reference point X become obvious in the following discussion.

Let the pressure in the cavity be changed by an amount $+ \Delta p/2$, producing a fringe intensity change from that at location X to that at B in Fig. 17. Alternatively, if the pressure

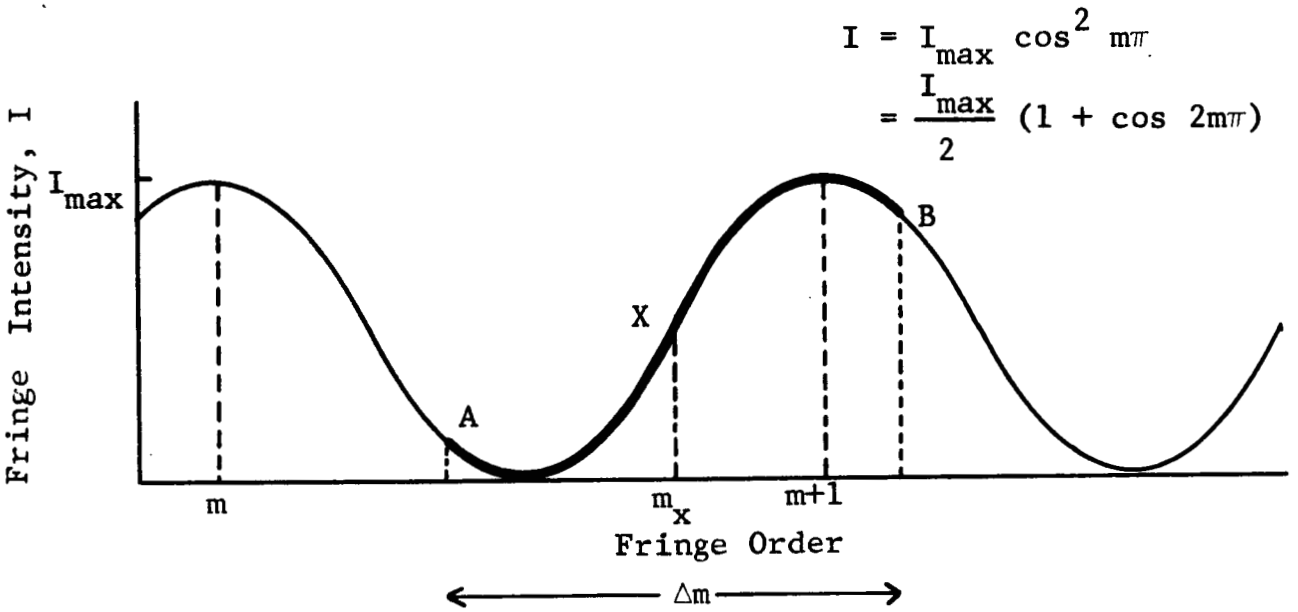

X Fringe order reference location

B Change in fringe order for pressure change $+\Delta p/2$

A Change in fringe order for pressure change $-\Delta p/2$

Δm Peak to peak fringe order change

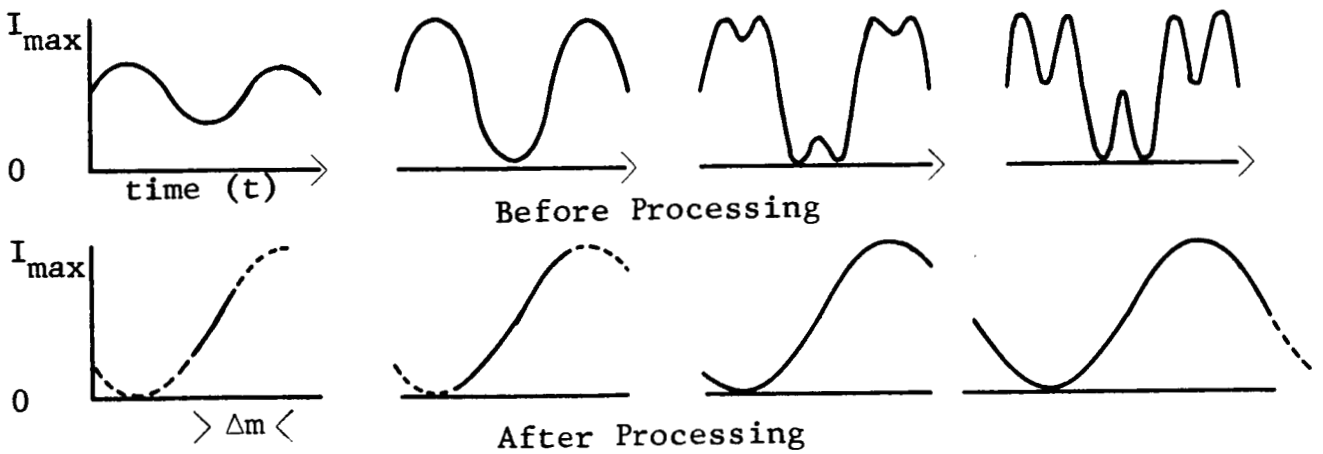

Fig. 17. Intensity Distribution of Fringe System and Detector Output Signals Before and After Processing.

in the cavity is changed by an amount $-\Delta p/2$, this would produce a fringe intensity change from that at location X to that at A. If these two pressure extremes are achieved alternately by applying an acoustic pressure signal of amplitude $\Delta p/2$ at a frequency f, it is readily seen that the photodiode detector will observe the intensity distribution over the region AXB on the intensity distribution curve and will cycle this curve AXB at the same frequency f. The peak to peak fringe order change Δm, corresponding to the peak to peak pressure change Δp, will be given by Eq. (13). Consequently, if the peak to peak fringe order change (Δm) can be determined by inspection of the photodiode detector output, the sound pressure level in the cavity can be determined.

Figure 17 also shows typical detector output signals as functions of time for different values of sound pressure level in the cavity. It can be seen at low sound pressure levels the detector output closely resembles a sinusoidal wave, but as the sound pressure levels increase so the output signal degenerates from a sinusoidal wave form. It is difficult by inspection of this output waveform on an oscilloscope to determine the peak to peak fringe order change, because ambiguities in signal interpretation are possible. However, inspection of the detector output signal as a function of time gives an indication of one possible method of signal interpretation. Since the fringe intensity follows a cosine squared distribution, we may write

$$I = I_{max} \cos^2 (m\pi)$$

or

$$I = \frac{I_{max}}{2} [1 + \cos (2m\pi)] \qquad (17)$$

Thus, when m is an integer, $I = I_{max}$, and when $(m + 1/2)$ is an integer, $I = 0$.

Maintaining the same reference point X on the fringe system, the order m_x at the location is such that $m_x + 1/4$ is an integer, n. If now an acoustic pressure is applied to the cavity following a sinusoidal time dependence, then the corresponding fringe order change will also follow a sinusoidal time dependence. Thus we have

$$\left.\begin{aligned} p(t) &= \frac{\Delta p}{2} \sin \omega t \\ m(t) &= \frac{\Delta m}{2} \sin \omega t \end{aligned}\right\} \qquad (18)$$

where

Δp = peak to peak acoustic pressure

Δm = peak to peak fringe order change.

Both signals p(t) and m(t) will be in phase because the pressure changes in the cavity produce instantaneous changes in the fringe system. We denote the time-dependent intensity observed by the detector as I(t). Thus

$$I(t) = \frac{I_{max}}{2} [1 + \cos 2 \left(m_x + m(t)\right) \pi] \qquad (19)$$

$$I(t) = \frac{I_{max}}{2} [1 + \cos 2m_x\pi \cos 2m(t)\pi - \sin 2m_x\pi \sin 2m(t)\pi] \quad (20)$$

But, since $m_x + 1/4 = n$ (an integer),

$$\cos 2m_x\pi = 0 \quad \text{and} \quad \sin 2m_x\pi = -1$$

Thus

$$I(t) = \frac{I_{max}}{2} [1 + \sin 2m(t)\pi] \quad (21)$$

$$= \frac{I_{max}}{2} \left[1 + \sin \left(2\pi \frac{\Delta m}{2} \sin \omega t\right)\right] \quad (22)$$

Equation (22) illustrates the complex nature of the time dependence of the intensity observed by the detector.

However, if the signal I(t) is applied to the Y-plates of an oscilloscope and a signal S(t) is applied simultaneously to the X-plates, where $S(t) = S \sin \omega t$, the resultant trace will have the form of a section of sine curve and will represent the actual fringe order excursion. The explanation follows: I(t) may be re-expressed in the form

$$I(t) = \frac{I_{max}}{2} \left[1 + \sin \left(\ell S(t)\right)\right] \quad (23)$$

where

$$\ell = 2\pi \frac{\Delta m}{2S}$$

If we neglect the steady D.C. component of this signal, the A.C. signal remaining is

$$\frac{I_{max}}{2} \left[\sin \left(\ell S(t)\right)\right] \quad (24)$$

If this signal is applied to the Y-plates while simultaneously S(t) is applied to the X-plates, the resultant trace must be a section of a sine curve because the signal applied to the Y-plates is proportional to the sine of the function $\ell \cdot S(t)$, where ℓ is a constant, independent of time, defined previously. The resultant trace corresponds to the curve AXB of the cosine squared distribution shown in Fig. 17. If the form of this distribution is re-expressed, as in Eq. (17), into a cosine curve, it can be demonstrated that both the oscilloscope trace and the curve AXB are identical sections of a complete sine or cosine wave. Consequently, the oscilloscope trace represents the actual fringe order excursion and enables determination of its value to be made easily and accurately.

Figure 17 shows a typical photodiode detector output displayed as a function of time and then processed in the manner described above. It can be seen that with this processing method the peak to peak fringe order change Δm can be readily observed.

To determine quantitatively the value of Δm, the following two methods are suggested.

Method 1

(a) Determine using illustrations a through e in Fig. 18 the approximate value of Δm by comparison with scope trace.

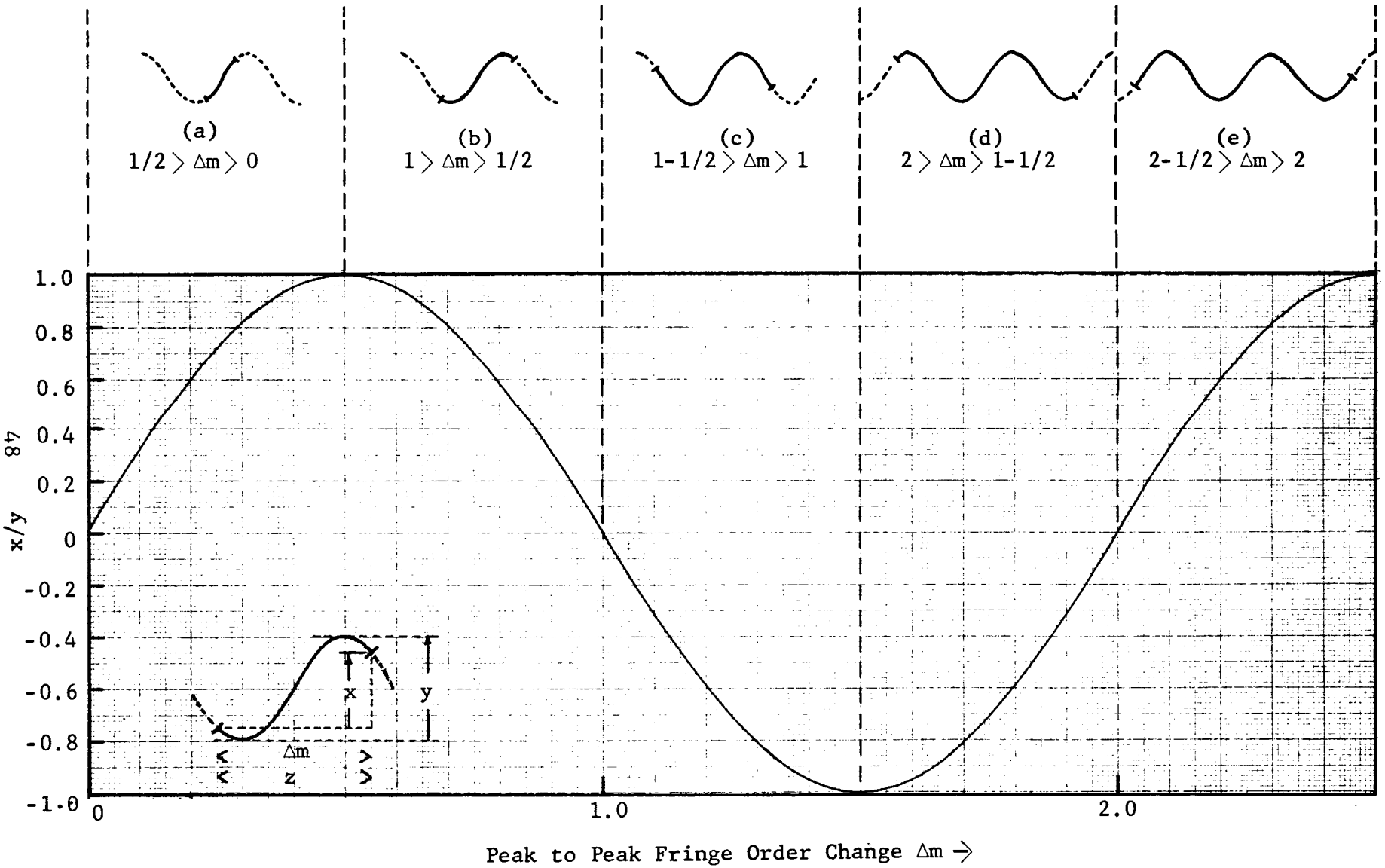

Fig. 18. Determination of Δm from Processed Signal.

(b) Determine the vertical separation of the end points of the trace x, shown in Fig. 18.

Then, for the value of x/y, the exact value of Δm can be taken from the graph shown in Fig. 18 by selecting the value in the correct Δm range. This graph was obtained by evaluating Eq. (17). The value of y, the fringe intensity peak to peak range, is determined prior to calibration by rotating the optical compensator and observing the peak to peak signal output while sweeping through the fringe system. It is important that the compensator remain in this sweep range when calibration is attempted because the fringe peak to peak signal output is a function of the optical beam's incident angle to the compensator.

Method 2

An alternative method of determining Δm, which can only be applied at high acoustic levels, consists of comparing the horizontal separation z (see Fig. 18) of the end-points of the processed signal to the horizontal separation between either adjacent minima and maxima or adjustment maxima (or minima). The separation between adjacent minima and maxima corresponds to a Δm of 1/2 and, between adjacent maxima (or minima), of 1.

Figure 16 shows the sound pressure level in the acoustic cavity given the value of Δm calculated as shown above. This was plotted from Eq. (16).

In the previous discussion of signal analysis, the use was made of a signal S(t). This signal could be supplied

through sampling the electrical input to the acoustic generator. Because it is necessary in the analysis that p(t) and S(t) are in phase, a phase adjustment may be required in the electrical signal to ensure a correct phase relationship and to enable a section of a sine curve trace to be obtained.

However, problems in signal interpretation could still be encountered. For example, if the acoustic pressure produced in the cavity, using an acoustic generator supplied with sinusoidal input, behaves in a nonlinear manner, then the assumption that $p(t) = (\Delta p/2) \sin \omega t$ will not be correct. Fourier analysis would show that p(t) has many components which are harmonics of the fundamental frequency. Consequently, m(t) would not be proportional to $\sin \omega t$ as assumed in Eq. (18), and therefore the A.C. component of I(t) would not be proportional to $\sin \ell \cdot S(t)$ as given by Eq. (24).

Consequently, displaying the A.C. component of I(t) on the Y-plates and S(t) on the X-plates would not produce a section of a sine curve, but instead a very complex trace whose interpretation may not be possible.

It is therefore suggested that, instead of using the electrical input signal to the generator as the processing signal S(t), the electrical output signal V(t) from the unknown transducer be utilized. If the transducer is an ideal device, the transducer output V(t) will be of identical form as p(t).

Consequently, Eq. (24) will still be valid if we replace S(t) by V(t). Then, maintaining the normal processing

method, i.e., applying the A.C. component of I(t) to the Y-plates and V(t) to the X-plates, a section of a sine curve will again be produced as an oscilloscope trace assuming correct phasing of the two signals in spite of the nonlinearity in acoustic signal.

If the transducer output V(t) is not of identical form as p(t), then this method of signal processing breaks down because of the complex oscilloscope trace which is produced. However, in this case, it is questionable whether any attempt to calibrate the transducer would be worthwhile. The fact that V(t) and p(t) are not identical implies that the transducer is not operating satisfactorily. Either one or both of the following conditions must exist:

(1) The dynamic range of the transducer has been exceeded, leading to signal distortion.

(2) The frequency response of the transducer is not uniform to sufficiently high frequencies to accommodate all harmonic components of the signal, if it is at all nonlinear.

If it is found that when the acoustic signal level is reduced (but still behaves nonlinearly) the processing method does enable a section of a sine curve to be produced, it can be assumed that the original difficulties in signal processing were due to overloading of the transducer. If no sine wave portion is produced, it can be assumed that the frequency

response of the transducer is not good in the region of the harmonics of the acoustic signal.

Thus, this signal-processing method enables a quick test to be made on the characteristics of the transducer.

Phase information can be determined by comparison of the signal I(t) and V(t) on an oscilloscope, or, at low acoustic signal levels, where I(t) has almost a sinusoidal form, using a phase meter.

V. PERFORMANCE EVALUATION OF CALIBRATION DEVICE

Upon completion of the final working device, a small test program was undertaken to check its performance. It was not possible in the time available to conduct an extensive program as was desirable. Consequently, calibration checks were only made using air in the acoustic cavity at atmospheric pressure. These checks were conducted at selected frequencies and intensities as could be generated using only the horn-driver units. An acoustic signal was generated in the acoustic cavity and the sound pressure level determined optically. This was checked against the level indicated by a Bruel and Kjaer 1/4 in. condenser microphone, Type 4136, located in the position in the cavity normally occupied by the transducer requiring calibration. The condenser microphone sensitivity was determined at the time of the tests using the Bruel and Kjaer pistonphone, Type 4220. This pistonphone supplies an acoustic calibrating signal accurate to $\pm$ 0.2 db at a single frequency of 250 c/s.

The levels in the cavity were determined optically using both methods of signal evaluation described in Section IV. Table II compares the levels determined optically with those measured with the 1/4 in. condenser microphone over the frequency range 520 c/s to 51 kc/s at sound pressure levels from 144 to 174 db. The deviation between the sound pressure level measured by the microphone and that determined using the interferometer is shown in Fig. 19. Data for method 1 and method 2

TABLE II

SOUND PRESSURE LEVELS IN THE CAVITY MEASURED USING
(a) THE INTERFEROMETRIC DEVICE AND
(b) A MICROPHONE CALIBRATED WITH A PISTONPHONE

Frequency (kc/s)	Method		SPL (Calibrated Microphone), in db: 144	149	154	159	164	169	174
			SPL (Optical Interferometer) and Deviation, in db						
0.52	1	SPL	143.8	148.6	154.7	158.8	162.4		
		Dev.	-0.2	-0.4	+0.7	-0.2	-1.6		
	2	SPL	143.6	148.6	154.0	158.2	162.0		
		Dev.	-0.4	-0.4	0	-0.8	-2.0		
1.67	1	SPL	143.8	148.7	153.9	159.0	163.4	168.8	174.0
		Dev.	-0.2	-0.3	-0.1	0	-0.6	-0.2	0
	2	SPL	143.6	148.8	153.6	159.0	163.8	168.4	173.0
		Dev.	-0.4	-0.2	-0.4	0	-0.2	-0.6	-1.0
3.90	1	SPL	144.8	149.1	153.6	159.0	163.4	168.6	
		Dev.	+0.8	+0.1	-0.4	0	-0.6	-0.4	
	2	SPL	145.0	148.8	153.6	158.7	163.6	168.4	
		Dev.	+1.0	-0.2	-0.4	-0.3	-0.4	-0.6	
6.2	1	SPL	143.2	148.6	153.8	159.2	163.8		
		Dev.	-0.8	-0.4	-0.2	+0.2	-0.2		
10.0	1	SPL	143.2	149.1	154.4	159.1			
		Dev.	-0.8	+0.1	+0.4	+0.1			
14.0	1	SPL	143.2	149.1	154.3				
		Dev.	-0.8	+0.1	+0.3				
18.5	1	SPL	143.2	148.7					
		Dev.	-0.8	-0.3					
23.8	1	SPL	142.6						
		Dev.	-1.4						
48.5	1	SPL	135.1						
		Dev.	-8.9						
51.0	1	SPL	134.4						
		Dev.	-9.6						
Symbols Used in Fig.			●	◇	◊	○	□	△	▽

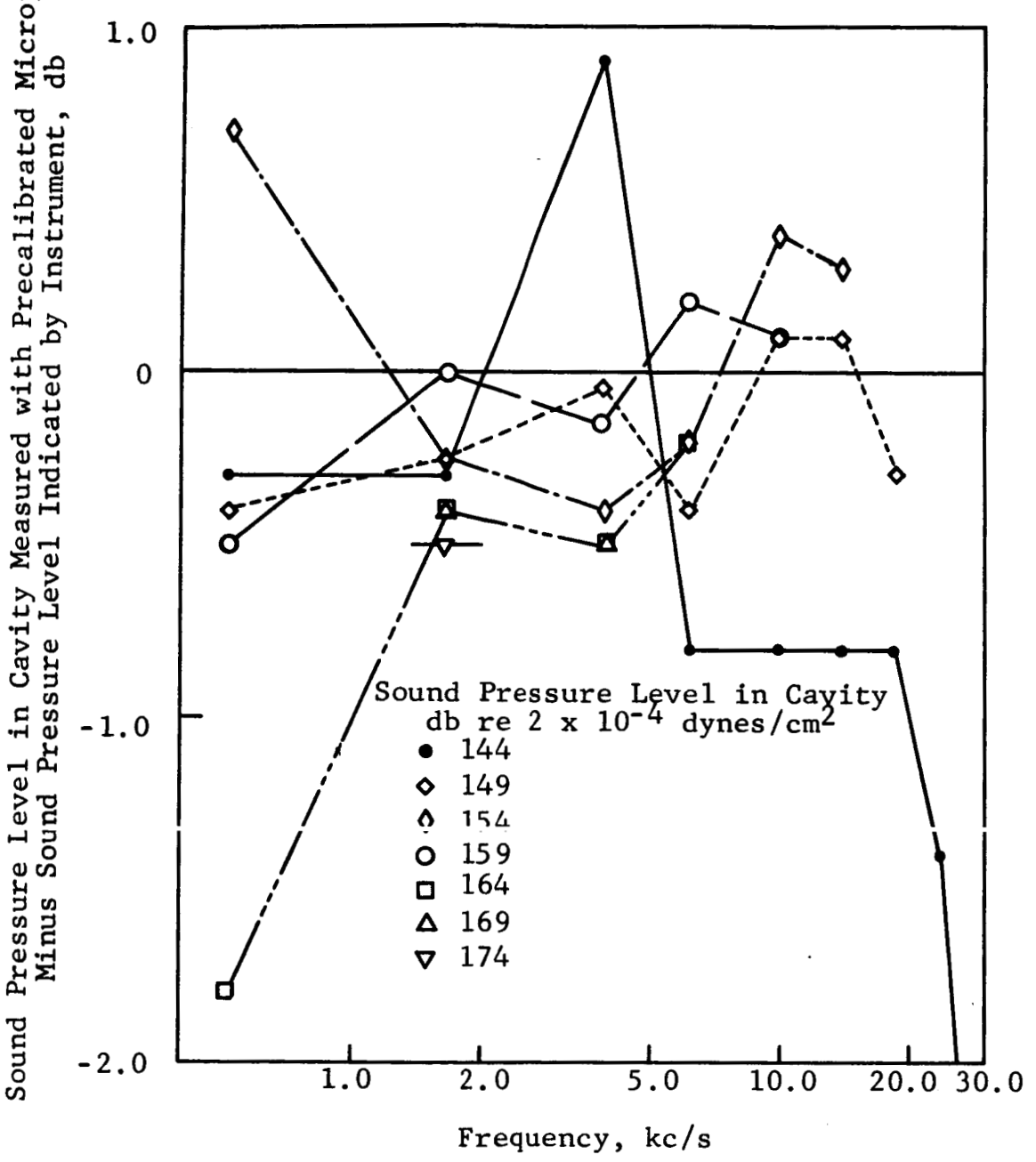

Fig. 19. Comparison of the Sound Pressure Levels in the Acoustic Cavity Measured with Precalibrated Microphone and Instrument.

has been averaged. It can be seen that the deviations appear to be independent of sound pressure level of the calibrating signal. The average deviations are less than 1/4 db. Individual deviations are generally less than 1/2 db. However, it can be seen that large deviations are experienced above a frequency of approximately 24 kc/s. This agrees with cross-mode determinations described in Section II. No phase comparisons were made because the microphone's specifications do not include phase information.

LIST OF REFERENCES

1. Whymark, R.R., "Magnetostrictive Transducers with Mechanical Loads," Acustica, Vol. 6, No. 3, p. 277, 1956.

2. Nowitzky, B.G., and Friedmann, W.M., "Die Erregung Von Schwingungen Mit Einer Grossen Schallintensität in Gasen Mittels Eines Magnetostriktiven Schallgebers," Fourth International Congress on Acoustics, Copenhagen, Paper No. N33, August 1962.

3. St. Clair, H.W., "An Electromagnetic Sound Generator for Producing Intense High Frequency Sound," Rev. Scien. Instruments, Vol. 12, pp. 250-256, May 1941.

4. Partington, J.R., "An Advanced Treatise on Physical Chemistry," Physico-Chemical Optics, Vol. 4, Longmans 1953.

5. Handbook of Chemistry and Physics, The Chemical Rubber Publishing Company, Cleveland, Ohio.

APPENDIX A

OPERATING MANUAL

1. INSTRUMENT LOCATION

Locate instrument on a level surface. To prevent transmission of external vibration to the interferometer, locate the legs of the instrument on soft rubber or polyurethane foam pads. Switch on laser. Ensure cover of interferometer is correctly positioned, so that the full extent of the laser beam enters the instrument. DO NOT LOOK DIRECTLY INTO LASER BEAM. Connect photodiode detector output cable to input of detector control. Switch on bias voltage and observe output on an oscilloscope. Undue vibration will produce an excessive noise level in the photodiode detector output. Interchange pads until the noise level is sufficiently reduced (to approximately 1 mV) to enable accurate signal determination. These adjustments should be made with the black cover on the interferometer and all openings to the interferometer system blocked to prevent turbulence effects producing additional noise level in the photodiode detector output. Switch off laser.

2. OPTICAL ADJUSTMENT

Under normal circumstances, no adjustments to the interferometer are required. Proceed to Step 3. Otherwise continue this section.

The fundamental conditions required in the adjustment procedures are that the reunited beams be parallel and coincident. The parallelism is more critical than the coincidence; the two fine adjustments are for the parallelism. Non-coincidence will result in interference only in the area of overlap of the beams with consequent reduction in the peak to peak signal output of the detector.

The parallelism condition is met if (1) the normals to the beam splitter and the mirrors are co-planar, and (2) the mirror normals make equal angles with the beam splitter normal. Adjustment H puts the normal of M1 into the plane defined by S and M2; adjustment V satisfies the angle condition (see Fig. 15).

If the mirrors were normal to the incident beams, the exit beams would now be coincident. With the small deviation from normal incidence employed here, it is additionally required that the path lengths between S and the mirrors be approximately equal.

It is also not required for parallel exit beams that the input beam from A1 be in the plane of the normals to the mirrors and beam splitter, but again a small departure will limit the permissable path difference between the arms of the interferometer.

There is no requirement that the input angle of incidence in the plane of the normals be 45°; the above discussion

applies for any physically realizable angle of incidence from 0° to 90°. It was chosen here as 45° for convenience in construction.

Optical Adjustment Procedure

Note: Coarse optical adjustment is required only if mirrors M1, M2 or splitter plate S have been recemented.

Fine optical adjustment is required only if the position of the metal blocks to which M1 and M2 are attached are disturbed.

All optical adjustments must be made with the acoustic cavity location in position so that the optical beam passes through the cell. In addition, when calibrations are being performed it is essential that the cell windows each face the directions that they face during adjustment procedures. Slight rotations of the cell are, however, permissible in the course of changing acoustic generators and transducers. Final cell window locations should be approximately (but not exactly) perpendicular to the optical beam. It is necessary to remove the black guard-plate from beneath the interferometer before coarse or fine adjustments are made. It is held in position by two Allen cap screws.

Coarse Adjustment

Coarse adjustment should be unnecessary unless M1, M2, or S has been recemented. However, if required, the following procedure should be followed.

1. Remove detector housing by removing the two mounting screws on horizontal centers, under snap cover. Set up a low power microscope objective, threaded end toward A3, to project an enlarged image of the exit beam cross-section 1/2 to 1 in. in diameter on a piece of paper a few inches away.
2. Block beam to M2 with a strip of opaque material. Rotate the M1 assembly about a vertical axis by loosening the three pedestal screws E. Set to displace the return beams to just miss A1.
3. Rotate beam splitter to produce exit beam through A3.
4. Unblock M2, block M1. Loosen the mounting screws for the M2 pedestal and rotate M2 to direct reflected beam through A2.
5. Unblock M1. Continue coarse adjustment of M2 until coarse fringes are observed. Re-tighten all mounting screws.

Fine Adjustment

If the fringes are vertical, adjust V in the direction that broadens them, until they swing horizontal. If the fringes are horizontal, adjust H in the direction that broadens them until they swing vertical. A condition is sought where the

fringe is much broader than the spot resulting in a near uniform intensity field of view. Perfect parallelism will not coincide with minimum intensity unless the optical compensator happens to be set for extinction at parallelism.

From the viewpoint of electrical signals, the objective of the adjustments is to maximize the peak to peak change in intensity upon a slow rotation of the compensator plate, i.e., ensuring that the fringes go from near zero extinction to maximum intensity.

3. LOCATION OF TRANSDUCER REQUIRING CALIBRATION

The main body of the acoustic cavity A (see Fig. A1) when in position in the interferometer, should normally be clamped tightly using cell clamping adjustment screw (see Fig. 14). Care must be taken, if the cavity is removed from the interferometer, so that the optical windows are not damaged or dirtied. Insert transducer T through knurled section B (which contains a small sunken O-ring). Screw section B to main body of cavity A, until finger-tight, so that transducer protrudes slightly (1/2 mm.) in section between optical windows. O-ring will then hold transducer in position. Locate section C with O-ring on lower end of main body A.

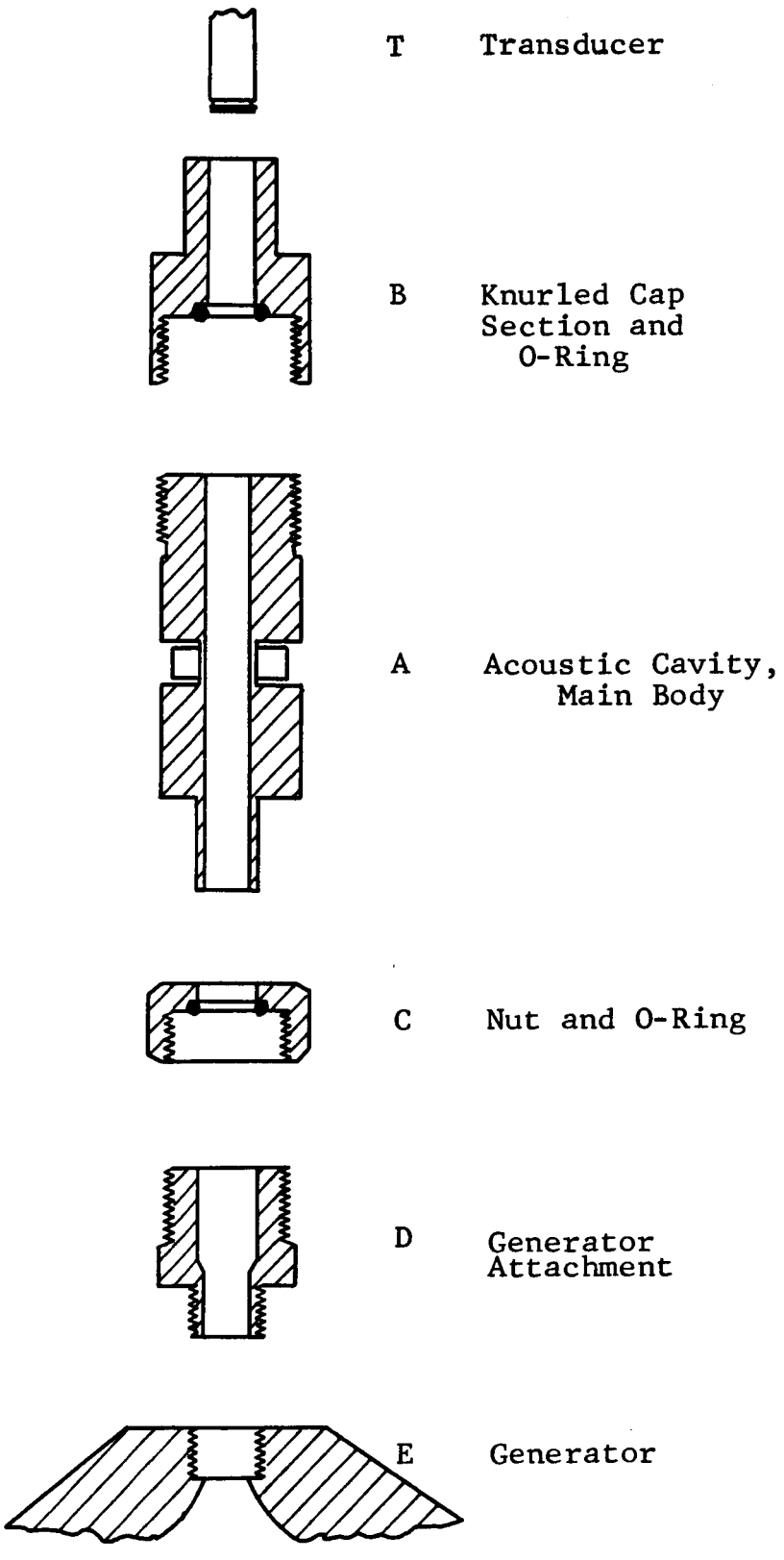

Fig. A1. Exploded View of Acoustic Cavity Assembly.

4. LOCATION OF ACOUSTIC GENERATOR

Screw section D into chosen acoustic generator. Locate generator on support platform beneath wooden support table. Adjust platform height and center generator until the lower end of A can nearly be positioned into D. Ensure generator is perfectly vertical. Loosen main body clamp and insert A into D with the optical windows approximately perpendicular to the laser beam path and tighten nut C. This process attaches the acoustic cavity to the acoustic generator.

Switch on laser beam and carefully change platform height (applying small adjustment to each of the three adjusting nuts in turn to maintain the complete system vertical and centrally located) until the laser beam passes through the optical windows just in front of the transducer face. (Ensure that it is the major beam passing through and not a secondary reflection. The major beam is the brightest.) Reclamp acoustic cell rigidly in position.

In the case of the St. Clair generator, connect up and operate a water cooling system, and fill cavity with helium.

Connect up generator electronics as shown in Fig. A2 and replace black cover over interferometer, again checking that the full extent of the laser beam enters instrument. Block any remaining gaps in base plate or in cover which would allow turbulent air to enter interferometer system.

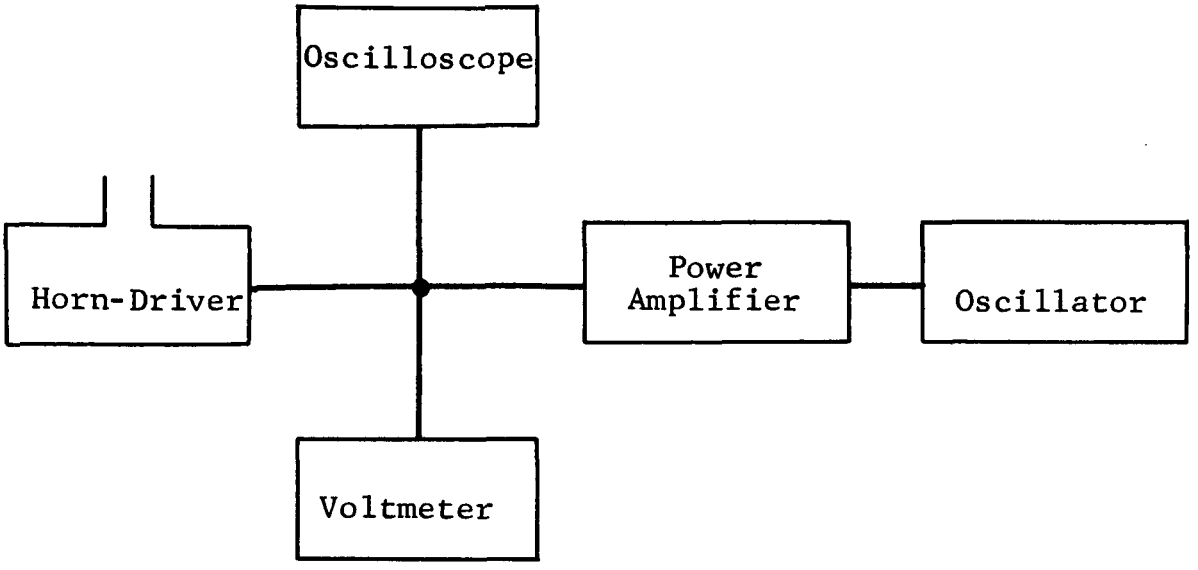

(a) Horn-Driver System

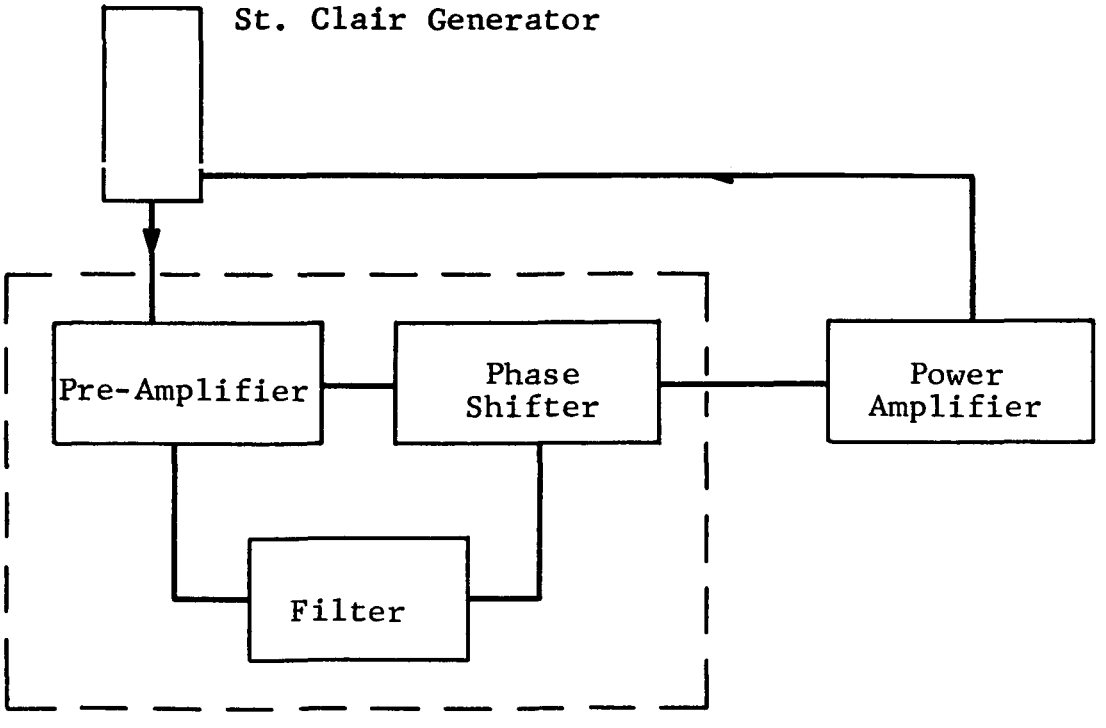

(b) St. Clair Generator System

Fig. A2. Generator Electronics.

5. CALIBRATION PROCEDURE

Rotate optical compensator very slowly in a region where it is perpendicular to the optical beam and observe an oscillatory signal on the oscilloscope (peak to peak value should be approximately 100 to 200 mV.). Adjust gain control until peak to peak signal trace occupies major portion of oscilloscope screen. Measure the peak to peak value 'y,' which represents the fringe's peak to peak intensity (see Fig. 18).

Apply power to the acoustic generator. Do not exceed the following voltages across the generators:

Jenson DD-100 ..... 50V

J. B. Lansing 075 ..... 13V

St. Clair Generators .. 25V

Finally, adjust compensator until detector output signal becomes symmetrical. (This adjustment is best performed at high intensities where the signal degenerates from a sinusoidal form into a complex wave form, see sample signals in Fig. 17.) This adjustment ensures that in absence of an acoustic signal the detector would observe the fringes at the location X as shown in Fig. 17.

Apply this signal to the Y-plates of the oscilloscope and to the X-plates apply either the electrical output of the unknown transducer or, less desirably, the electrical input to the acoustic generator. The chosen X-plate signal must be applied through the phase shifter device which must be adjusted

until the resultant oscilloscope trace resembles a section of a sine wave. (It is not essential for perfect reduction of the trace into a sine wave.) Check that the signal is symmetrical. Otherwise further fine adjustment of the compensator is required. Measure the vertical separation of the end points of the trace 'x' (see Fig. 18). Compute the fraction x/y and from Fig. 18 determine the value of Δm. The sound pressure level in the cavity can then be obtained using this value of Δm from Fig. 16.

An alternative method of determining Δm which can only be applied at high intensities follows.

Determine the horizontal separation of the end-point of the oscilloscope trace 'z' (see Fig. 18). Measure the horizontal separation 'h' between a maxima and minima of the trace. This length corresponds to $\Delta m = 1/2$. Then the unknown Δm is equal to z/2h. As before, use Fig. 16 to determine the sound pressure level.

Phase determination may be accomplished by comparing the transducer output to the detector output on a dual beam oscilloscope or using a phase meter.

APPENDIX B

OPTICAL COMPONENT SPECIFICATIONS

Detector EG&G; SD-100 photodiode
(NB, the lead closest to the tab must be biased positive. Maximum voltage 150V)

Laser Spectra-Physics, 130B, helium-neon gas laser

Beam splitter 1/8 x 9/16 x 5/8 in.

Mirrors (front surface aluminum) 1/2 x 1/2 x 5/8 in.

Cell windows 3.2, 3.2+1, x 3 x 7 mm. (see sketch)

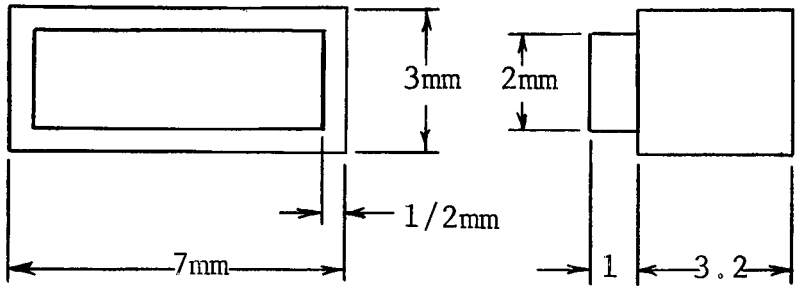

Stationary plate 1/8 x 9/16 x 5/8 in.

Optical compensator 1/8 x 1/2 x 1 in.

Adhesives:

Cell windows--hard Canada balsam

Other--rosin-beeswax 7:1*, black spiezon stick wax

---

*Worked best on aluminum.